

BSc Altijana Hromic

**Characterisation of H174N of berberine
bridge enzyme from
*Eschscholzia californica***

MASTER THESIS

zur Erlangung des akademischen Grades
Master of Science (MSc)

erreicht an der
Technischen Universität Graz

Betreuerung: Univ.-Prof. Mag. *rer. nat.* Dr. *rer. nat.* Peter Macheroux
Dr. Silvia Wallner
Institut für Biochemie
Technische Universität Graz

Graz, 2012

dedicated in love to my parents

Acknowledgements

I would like to express my gratitude to my dear parents and rest of my family, especially my aunt Erna, for helping me and supporting me through my studies and for always believing in me. I also want to thank them for enabling my studies at the university.

Furthermore, I would like to express my gratitude to Prof. Dr. Peter Macheroux for offering me the position as master student in his group and for giving me the opportunity to work on an interesting research project. Moreover, I want to thank him for his continuous support throughout the whole project.

I would also like to thank all my friends and my dear colleagues for their suggestions and great lab atmosphere, which made my work on this project more enjoyable.

Special thanks to Silvia Wallner, Bastian Daniel, Alexandra Binter, Barbara Steiner, Martina Zandl and Karin Koch for motivating me in those days where I thought that I lost all motivation and inspiration.

Thank you for believing in me and for telling me to be always optimistic.

Declaration

I declare that the thesis entitled “Characterisation of H174N of berberine bridge enzyme from *Eschscholzia californica*” is my own work, that it has not been submitted for any degree of examination in any other university, and that all the resources I have used or quoted have been indicated and acknowledged by complete references.

Altijana Hromic, January 2013

Eidesstattliche Erklärung

Ich erkläre an Eides statt, dass ich die vorliegende Arbeit selbstständig verfasst, andere als die angegebenen Quellen/Hilfsmittel nicht benutzt, und die den benutzten Quellen wörtlich und inhaltlich entnommene Stellen als solche kenntlich gemacht habe.

Altijana Hromic, Januar 2013

Abstract

Flavoproteins are a large group of proteins that use FAD or FMN for catalysis. In most flavoproteins the cofactor is non-covalently bound, however both monocovalent and bicovalent attachment modes are also known. Bicovalent flavinylation gives the respective enzymes a lot of interesting properties, such as a high redox potential. Moreover, bicovalent linkage can be crucial for holding the flavin cofactor in the active site and for structural integrity.

Berberine bridge enzyme (BBE) belongs to the class of bicovalently flavinylated oxidases. It is a fundamental enzyme of alkaloid biosynthesis in specific plant families like *Berberidaceae* or *Papaveraceae*. BBE catalyses the oxidative ring closure of the *N*-methyl group of (*S*)-reticuline to the C8 atom of (*S*)-scoulerine.

One important active site residue in BBE is His174. It was identified as crucial because of its role in stabilisation of the reduced state of the flavin cofactor.

In this work I present the biochemical characterisation of a BBE His174Asn variant. From sequence alignments it is known that His174 of BBE is strictly conserved among bicovalently linked flavoprotein oxidases and that an asparagine residue is present at the respective position of bicovalently flavinylated dehydrogenases (like Phl p 4 and TrdL). Biochemical parameters like redox potential and turnover rates were determined and compared with wild type BBE and BBE His174Ala. An approximately seven-fold decrease in catalytic activity and a two-fold decrease in redox potential was determined for His174Asn in comparison with BBE wild type. A possible reason for this decrease is absence of a hydrogen bonding network between His174 and the isoalloxazine ring system of flavin cofactor when His174 is replaced with Asn. Therefore, a crystal structure of the His174Asn variant would be necessary to prove this hypothesis.

Kurzfassung

Flavoproteine sind eine Enzymklasse, die einen FMN oder einen FAD Kofaktor für die Katalyse besitzen. Der erste charakterisierte Vertreter der bivalent verknüpften Flavoproteine war Glucosylglycosyltransferase deren Struktur im Jahr 2005 aufgeklärt wurde. Weiterhin ist die bivalente Verknüpfung wichtig für strukturelle Integrität des Proteins und für die richtige Positionierung des Flavins im aktiven Zentrum. Diese Proteine haben spezielle Eigenschaften, wie zum Beispiel ihr hohes Redoxpotential.

Berberine bridge enzyme (BBE) gehört in die Gruppe der bivalent verknüpften Flavoproteine. BBE ist in der Lage die oxidative Zyklisierung der *N*-Methylgruppe von (*S*)-Reticuline zum C8 Kohlenstoffatom von (*S*)-Scoulerin durchzuführen.

In BBE wurde His174 als wichtige Active Site Aminosäure identifiziert. His174 ist involviert in die Stabilisierung von negativen Ladungen am Flavinring während Kofaktorreduktion.

Im Rahmen dieser Arbeit wurde eine biochemische Charakterisierung der Variante His174Asn von BBE durchgeführt. Es ist bekannt das einige Flavoproteine Histidin auf Position 174 haben und sind dementsprechend Oxidasen. Andere Gruppe von Flavoproteinen haben auf der gleiche position Asparagine und sind Dehydrogenasen. Die Hauptaufgabe des Projektes war Oxidase in eine Dehydrogenase umzuwandeln durch Austausch von beteiligten Aminosäuren.

Biochemische Parameter wie Redoxpotential und katalytische Aktivität wurden bestimmt und mit BBE WT und BBEHis174Ala verglichen. Eine 7-fache Abnahme in der katalytischen Aktivität sowie eine 2-fache Abnahme des Redoxpotentials wurde im Vergleich zu BBE WT erhalten. Diese Abnahme des Redoxpotentials und von k_{cat} könnte auf ein Fehlen eines stabilisierenden Wasserstoffbrückennetzwerks am N(1)-C(2)=O Lokus zurückgeführt werden, welches durch den Austausch von His174 entsteht.

Table of Contents

List of Abbreviations	x
1 Introduction	1
1.1 Alkaloids	1
1.1.1 General aspects	1
1.1.2 Benzyloquinoline alkaloids	2
1.1.3 Benzyloquinoline alkaloid biosynthesis	2
1.1.4 Pharmacology of benzyloquinoline alkaloids	4
1.2 Flavoproteins	5
1.2.1 Introduction into flavoproteins	5
1.2.2 Covalent flavinylation	7
1.3 Classification of flavoproteins	7
1.3.1 Dehydrogenases	8
1.3.2 Reductases	8
1.3.3 Oxidases	9
1.3.4 Monooxygenases	9
1.3.5 Disulfide Oxidoreductases	9
1.3.6 Non-redox flavoproteins	10
1.3.7 Flavoproteins with bicovalently linked cofactors	10
1.4 Oxygen reactivity of flavoproteins	11
1.5 Berberine bridge enzyme (BBE)	13
1.5.1 General introduction	13
1.5.2 Strategies for BBE expression	17
1.5.3 Aims of the thesis	18
2 Materials	19
2.1 Culture media	19
2.2 Buffers and solutions	20
2.2.1 Buffer and gel for agarose gel electrophoresis	20
2.2.2 Buffers for western blot	20
2.2.3 Buffers for protein purification	21
2.2.4 Other buffers	21
2.3 Standards	21

2.4	Kits	21
2.5	<i>Pichia</i> strains	22
2.6	Primers.....	22
2.7	Vectors.....	22
2.8	Equipment.....	23
3	Methods	24
3.1	Standard methods	24
3.2	Plasmid isolation	24
3.3	Restriction.....	24
3.4	Ligation.....	24
3.5	Transformation into <i>P. pastoris</i>	25
3.6	Site directed mutagenesis	25
3.6.1	Expression in 96-deep-well plates.....	25
3.6.2	Expression in 300 mL shake flasks	26
3.6.3	Expression in 2L baffled flasks	26
3.7	Dot-Blot.....	26
3.8	Sodium dodecyl sulphate-polyacrylamide gel electrophoresis	27
3.9	Western Blot.....	28
3.9.1	Colony PCR.....	28
3.9.2	Large-scale expression	29
3.10	Protein purification.....	29
3.11	Activity assays.....	30
3.12	Anaerobic photoreduction	30
3.13	Steady-state kinetic analysis.....	31
3.14	Determination of redox potential.....	31
3.15	Crystallization.....	32
4	Results	33
4.1	Cloning, expression and purification	33
4.1.1	Site-directed mutagenesis	33
4.1.2	Screening	34
4.1.3	Small-scale expression	35
4.1.4	Bioreactor fermentation.....	36
4.1.5	Protein purification.....	38
4.2	Protein characterisation	43

4.2.1	Anaerobic photoreduction	43
4.2.2	Steady-state kinetic analysis	45
4.2.3	Redox potential determination.....	47
4.2.4	Observation of flavin degradation	48
4.2.5	Crystallization.....	49
5	Discussion	51
6	Conclusion	55
7	Appendix 1	56
7.1	Introduction	57
7.2	BBE-like proteins in plants	57
7.3	Conclusion	60
7.4	Results	61
8	Appendix 2	63
8.1	List of tables	64
9	References	65

List of Abbreviations

AA	acrylamide
Abs	absorbance
Asn	asparagine
BBE	berberine bridge enzyme
<i>E. coli</i>	<i>Escherichia coli</i>
DNA	deoxyribonucleic acid
DTT	dithiothreitol
EDTA	ethylenediamine tetraacetic acid
fwd	forward
HIC	hydrophobic interaction chromatography
kDa	kilo Dalton
LB	Luria-Bertani broth
min	minutes
OD ₆₀₀	optical density measured at a wavelength of $\lambda = 600$ nm
<i>P. pastoris</i>	<i>Pichia pastoris</i>
rev	reverse
SDS	sodium dodecyl sulphate
SDS-PAGE	sodium dodecyl sulphate-polyacrylamide gel electrophoresis
sec	seconds
TEMED	<i>N,N,N'N'</i> -tetramethylethylenediamine
TRIS	2-amino-2-(hydroxymethyl)propane-1,3-diol

1 Introduction

1.1 Alkaloids

1.1.1 General aspects

Alkaloids are a large and diverse group of nitrogen containing compounds. They are common secondary metabolites in more than 20% of all plant species, where they play an important role in defence against herbivores and pathogens. In medicine, a great number of alkaloids is used as stimulants, toxins and narcotics (Facchini *et al.*, 2005).

About 25% of all known pharmaceuticals nowadays in use are isolated from plants in form of extracts, teas or as purified substances with biological activity (Tyler *et al.*, 1994).

Alkaloids are derived from different amino acids, like histidine, tryptophan, lysine, or tyrosine (Minami *et al.*, 2008).

Corresponding to the structural characteristics, alkaloids are divided into different groups like (benzyl)isoquinoline, indole, purine, tropane, and quinolizidine type alkaloids (Facchini *et al.*, 2005).

Due to their complex structure, total organic synthesis is not possible for many of these alkaloids and their extraction from natural sources results in low yields of purified biologically active substances (Facchini *et al.*, 2001).

Nowadays, different new methods for the production of alkaloids exist. Some of them use transgenic plants for improved accumulation of pathway intermediates. Others use metabolic engineering of microbial host organisms to make platforms for fermentative production of different plant alkaloids (Minami *et al.*, 2008).

1.1.2 Benzyloisoquinoline alkaloids

Benzyloisoquinoline alkaloids (BIAs) are a large group of alkaloids comprising more than 2500 determined structures (Facchini *et al.*, 2001).

This group of alkaloids is derived from tyrosine in a series of different chemical reactions like decarboxylation, reduction, methylation, hydroxylation, and intramolecular coupling (Liscombe, 2008).

They all utilise the same isoquinoline heterocycle as common structural feature.

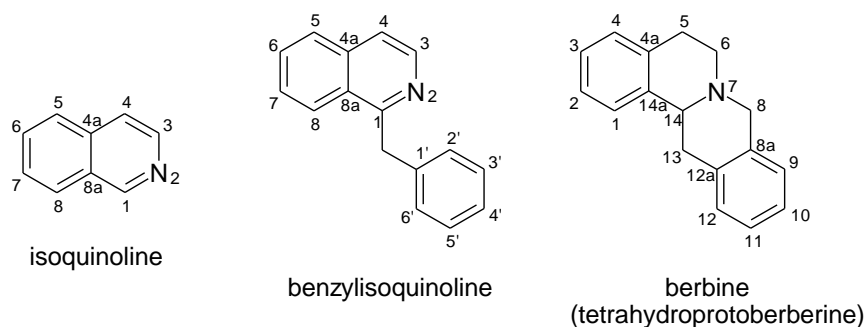


Figure 1: Structure and numbering conventions of benzyloisoquinoline alkaloids (Liscombe, 2008).

Benzyloisoquinoline alkaloids are produced in basal angiosperms of the order of Ranunculales, like in *Berberidaceae*, *Papaveraceae* and *Ranunculaceae* (Liscombe, 2008; Liscombe, 2005).

For investigating berberine biosynthesis different model systems like California poppy (*Eschscholzia californica*), opium poppy (*Papaver somniferum*) and yellow meadow rue (*Thalictrum flavum*) were used (Liscombe, 2008).

1.1.3 Benzyloisoquinoline alkaloid biosynthesis

Biosynthesis of benzyloisoquinoline alkaloids begins with the condensation of dopamine and 4-hydroxyphenylacetaldehyde, which both are derived from L-tyrosine (Samanani *et*

al., 2004). This first step leading to the formation of (*S*)-norcoclaurine is catalyzed by norcoclaurine synthase (NCS) (Facchini *et al.*, 2007). (*S*)-Norcoclaurine is further transformed to (*S*)-reticuline in a series of methylation and oxidation reactions catalyzed by norcoclaurine 6-*O*-methyltransferase (6OMT), coclaurine *N*-methyltransferase (CNMT), *N*-methylcoclaurine 3'-hydroxylase (NMCH), and 3'-hydroxy-*N*-methylcoclaurine 4'-*O*-methyltransferase (4'OMT) (Facchini *et al.*, 2005).

(*S*)-reticuline is an important branch point intermediate in benzyloisoquinoline alkaloid biosynthesis. It can undergo diverse enzymatic reactions leading to the formation of morphinan, benzophenanthridine, protoberberine, and aporphine alkaloids (Liscombe, 2008).

(*S*)-reticuline is converted to (*S*)-scoulerine through the action of berberine bridge enzyme (BBE). BBE catalyzes the oxidative intramolecular C-C bond formation thereby creating the so called "berberine bridge" (Steffens *et al.*, 1984). This reaction is the committed step in the biosynthetic routes leading to the formation of protopine, protoberberine, and benzophenanthridine alkaloids (Liscombe, 2008).

In figure 2 BBE is marked with the EC number 1.21.3.3, catalysing the conversion of (*S*)-reticuline to (*S*)-scoulerine.

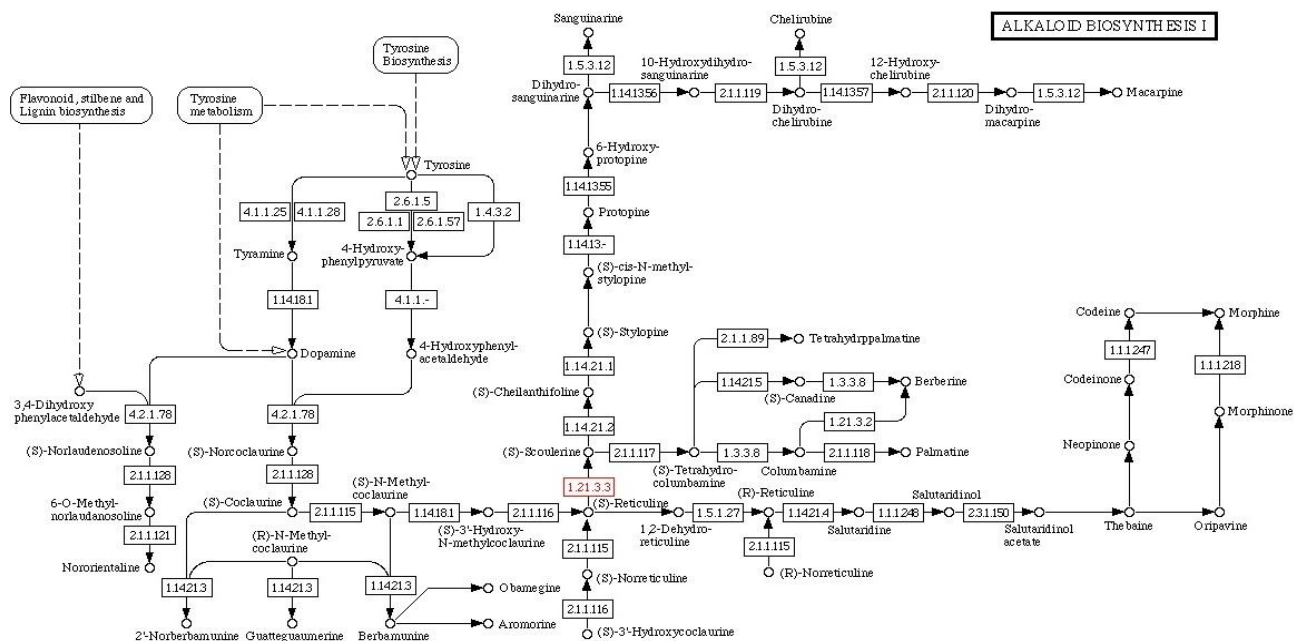


Figure 2: Summary of alkaloid biosynthesis.

(Source: <http://salmonellabase.com/pathway.php?vGenomeId=24>)

1.1.4 Pharmacology of benzyloquinoline alkaloids

Benzyloquinoline alkaloids are an interesting group of alkaloids which show a wide range of different pharmacological activities (Facchini, 2001).

Pharmacological characteristics of alkaloids were recognized very early, which led to a wide use of alkaloid containing plants and extracts in different areas of alternative medicine.

Among the benzyloquinoline alkaloids (*S*)-reticuline was shown to have major effects on the central nervous system (Morais *et al.*, 1998).

The plant *Nelumbo nucifera* is very common in oriental medicine. It is an aquatic crop which contains (*R*)-coclaurine and (*S*)-noncoclaurine, that can be used for the treatment of fever, sweating, and strangury (Kashiwada *et al.*, 2005).

Pseudocoptisine is a quaternary alkaloid with a benzyloquinoline skeleton. This alkaloid is a major active compound in *Corydalis* species and it shows anti-amnesic effects (Hung *et al.*, 2008).

It is also important to mention that different *Machonia* species contain an high elevated amount of protoberberine alkaloids, which are used in alternative medicine as antipyretic and analgesic drugs (Chao *et al.*, 2009).

A general pharmacological property of many benzyloquinoline alkaloids is their antispasmodic activity. This is caused by inhibition of Ca^{2+} transport as reported by Anselmi *et al.*, 1992.

The most important effect of a large number of berbine alkaloids is their activity on the central nervous system. Different studies with mice and rats showed that some berbine alkaloids show a strong sedative potential.

Furthermore it was demonstrated that some protoberberines like palmatine and coptisine have a high potential for preventing Alzheimer`s disease (Mo *et al.*, 2007).

Recently, the effect of (*S*)-stepholidine and (*S*)-chloroscoulerine on the dopaminergic system was shown. This makes those compounds potential drugs in the treatment of

different stages of schizophrenia and symptoms characteristic for Parkinson`s disease (Mo *et al.*, 2007).

1.2 Flavoproteins

1.2.1 Introduction into flavoproteins

Flavoproteins were first mentioned in 1879, when studies on the composition of cow`s milk resulted in the isolation of a bright-yellow pigment. At that time this pigment was termed lactochrome. By the early 1930s, this same pigment has been isolated from a range of sources, and recognised as a component of the vitamin B complex. Its structure was determined almost simultaneously by two groups in 1934, and given the name riboflavin, derived from the ribityl side chain and the yellow colour of the conjugated ring system (Massey, 2000.)

Riboflavin (Vitamin B₂) is a precursor for FMN and FAD in almost all organisms. The redox-active isoalloxazine ring system is employed as coenzyme in different enzymatic reactions (Macheroux *et al.*, 2011).

More than 90% of flavin-dependent enzymes belong to the group of oxidoreductases, which catalyse oxidation, reduction or dehydrogenation reactions. Furthermore this cofactor can be found in enzymes classified as transferases, lyases, isomerases, or ligases. Flavin cofactors play also an important role in many biological pathways. They are responsible for signalling and sensing molecules in phototropism and nitrogen fixation (Macheroux *et al.*, 2011).

The major group of enzymes employ FAD (75%) rather than FMN (25%) as non covalently bound cofactor (90%). FAD-containing enzymes bind the cofactor in a Rossmann fold. On the other hand, FMN-containing enzymes preferably adopt a ($\beta\alpha$)₈- (TIM)-barrel-like or flavodixin-like fold (Macheroux *et al.*, 2011).

The yellow vitamin B₂ can be found in many bacteria and plants. It is converted to FMN or FAD by riboflavin kinase, followed by further adenylation via FAD-synthetase in two ATP-dependent reactions.

The complexity of most flavin-catalysed reactions is increased when the enzyme binds additionally other redox-active cofactors, such as iron-sulfur clusters or others like heme or thiamine diphosphate (Macheroux *et al.*, 2011).

Some enzymes have their cofactor covalently bound to the active site. Covalent attachment of FMN occurs extremely rare in comparison with enzymes that have FAD in their active site.

Today different types of covalent attachment of the flavin cofactor are known, which are shown in figure 3. Those types can be divided into two subgroups: one where the cofactor is linked via its 8- α -methyl group and one with a linkage involving the C6 atom of the isoalloxazine ring system. The former can be further subdivided depending on the amino acid side chain attached to the flavin. Attachment can occur either via histidine, cysteine, tyrosine or an aspartate (CmlS) residue. Up to now only cysteinylolation was found as covalent attachment to the C6 carbon of the isoalloxazine ring (Mewies *et al.*, 1997).

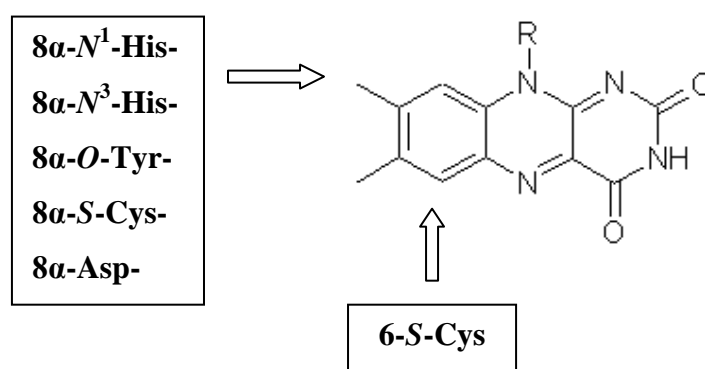


Figure 3: Types of covalent flavin linkage found in flavoenzymes.

Moreover, bicovalent attachment of the cofactor was found in flavoproteins belonging to the *p*-cresolmethylhydroxylase (PCMH) superfamily. Here the cofactor is attached to the

enzyme via the 8 α -position and C6 atom of the isoalloxazine ring system (Macheroux *et al.*, 2011). Important member of this class is BBE.

1.2.2 Covalent flavinylation

The mechanism of covalent flavinylation was studied for proteins with monocovalently tethered flavins. In all cases flavinylation is described to occur autocatalytically. For a huge number of investigated proteins similar mechanisms for covalent flavin coupling at the C8 α were suggested.

The mechanism starts with proton abstraction from the C8 methyl group of the flavin with subsequent stabilization of the negative charge at the N(1)-C(2)=O locus of the isoalloxazine ring. This stabilization can be attributed to a positive amino acid residue such as a lysine in monomeric sarcosine oxidase or an arginine in *p*-cresol methylhydroxylase and vanillyl-alcohol oxidase. Until now no bicovalently flavinylated protein has been investigated with regard to mechanistic aspects of bicovalent flavin attachment (Wallner *et al.*, 2012a).

First mutagenesis studies showed that both covalent linkages seem to form independently of each other because both histidinylated and cysteinylated single variant proteins could be expressed and isolated.

1.3 Classification of flavoproteins

A classification of flavoproteins can be done according to different criteria, like their preferred substrates, their topology, or the reactions catalysed. Since the redox-active flavin cofactor can be employed for the catalysis of various reactions, flavoproteins are here classified according to their catalytical function.

1.3.1 Dehydrogenases

Members of this group catalyse the transfer of electrons between different substrates. Despite of that, they are totally unreactive with molecular oxygen. Electrons from substrate oxidation are transferred to specific carriers such as NADP⁺ (electron acceptor). Well studied examples for dehydrogenases are e.g. acyl-CoA dehydrogenases reviewed by Ghisla and Thorpe (2004). Today there are also examples for dehydrogenases with a bicovalently attached FAD-cofactor. One representative of this class is Phl p 4, a major allergen in timothy grass. Phl p 4 possesses an asparagine residue on a crucial position near the N(1)-C(2)=O locus, where oxidases have a conserved histidine.

Another bicovalently flavinylated dehydrogenase is TrdL. Different *in vivo* and *in vitro* experiments showed that TrdL is a FAD-dependent dehydrogenase, responsible for C-10 keto formation (Mo *et al.*, 2011).

1.3.2 Reductases

In comparison to dehydrogenases, reductases use the electrons from an electron donor (NADH) to reduce an organic substrate. A typical reductase is the old yellow enzyme (OYE). It was first isolated from brewers' bottom yeast by Warburg and Christian (1932) and consists of a colourless apoprotein and a yellow dye, both essential for enzyme activity. The discovery of OYE components helped to explain the essential role of proteins in enzyme catalysis (Zhu *et al.*, 2012).

1.3.3 Oxidases

Enzymes of this group are capable of oxidising organic substrates directly in a two electron transfer. This step is followed by reoxidation of the flavin by molecular oxygen.

According to literature, two possibilities exist for a two electron transfer from the organic substrate to the flavin molecule. The first one is a direct transfer of a hydride, as it appears to be the case for alcohol oxidase and BBE (Fraaije and Mattevi, 2000). The second possibility is a radical mechanism, where the flavin is reduced by two subsequent one electron transfers as proposed for the oxidation of amines. The following oxidative half reaction, which is typical for all oxidases, then generates hydrogen peroxide via direct transfer of two electrons to O_2 (Edmondson, 1995).

1.3.4 Monooxygenases

Enzymes of this class also react with molecular oxygen. In contrast to oxidases, no hydrogen peroxide is generated. Instead, one half of O_2 is inserted into an organic substrate where the other half is set free in form of H_2O . The electrons needed for such a conversion can be either provided by the substrate itself, like internal monooxygenases or, as it is the case for most members of this class, through specific external electron donors such as NADH or NADPH (external monooxygenases) (Massey, 2000).

1.3.5 Disulfide Oxidoreductases

This family of enzymes contain an active-site disulfide in addition to the FAD prosthetic group. They use pyridine nucleotide as one substrate, and disulfide or dithiol is used as other substrate.

These enzymes play a crucial role in protection against cellular damage by radical oxygen and in cellular energy metabolism. The reaction mechanism involves the reduction of the flavin by NAD(P)H and a subsequent transfer of electrons to the active site disulfide

bridge. The generated cysteines perform an exchange reaction with disulfide substrates like thioredoxin or glutathione (Massey, 2000).

1.3.6 Non-redox flavoproteins

In addition to the groups of flavoproteins mentioned before, there exist some flavoproteins which are involved in reactions without any changes in redox state of the flavin cofactor. One member of this group is chorismate synthase studied by Kitzing *et al.* (2004). Here only an intermediate transfer of electrons from the flavin to the substrate is crucial for the catalytic mechanism. Another example is hydroxynitrile lyase from *Prunus amygdalus*. This enzyme contains a FAD cofactor near the active site, which is probably too far away to participate in a redox reaction. In this case a structural role and the supply of a mandatory electrostatic environment for the reaction is proposed by Dreveny *et al.* (2002).

1.3.7 Flavoproteins with bicovalently linked cofactors

As mentioned before, the flavin cofactor can also be bicovalently attached to the 8 α -position and C6-position of the isoalloxazine ring system. It has been shown that enzymes with bicovalently linked cofactors are capable of catalysing important and challenging chemical reactions in eukaryotic as well as in prokaryotic systems. Today no examples of bicovalently linked flavoproteins exist in archea and the animal kingdom and sequence alignments suggest the absence of bicovalently attached flavoproteins in these species (Wallner *et al.*, 2012).

Nowadays, the number of enzymes known to have both covalent cysteinylolation and histidinylolation of the flavin is increasing.

The revolutionary year was 2005, where the crystal structure of glucooligosaccharide oxidase (GOOX) gave the first example of a bicovalently linked FAD cofactor (Huang *et al.*, 2005). Here the FAD cofactor is clearly linked to a histidine and a cysteine residue at

the 8 α -methyl and C-6 position of the flavin, respectively. The monocovalent attachments in this flavoprotein are combined to form a bicovalently linked flavin.

Bicovalent flavin attachment can have several purposes for the flavoenzyme. Bicovalent flavinylation shifts the redox potential of the cofactor hence making substrate oxidations possible. Moreover, covalent flavinylation can be crucial for holding the flavin cofactor in the active site.

These factors play an important role in chitooligosaccharide oxidase (ChitO) from *Fusarium graminearum*, where bicovalent flavinylation effects the redox potential and where it effects the correct positioning of the cofactor in the open active site of the enzyme. Moreover, bicovalent flavinylation can be crucial for the formation of a catalytically competent Michaelis-Menten-complex (Heuts *et al.*, 2008).

Furthermore, bicovalent linkage is important for structural integrity as obvious from low protein yields when covalent linkages are removed (Winkler *et al.*, 2009).

1.4 Oxygen reactivity of flavoproteins

Many flavoproteins like oxygenases and monooxygenases react more rapidly with oxygen than free flavins. There are many suggestions of how enzymes are capable of enabling this fast reaction (Palfey *et al.*, 2011).

The reaction of reduced flavin and molecular oxygen in solutions is slow since spin inversion is required for the reaction of the reduced flavin (singlet) with O₂ (triplet) to form H₂O₂ and oxidized flavin. The whole reaction happens by electron transfer from the reduced flavin to O₂ creating a charged radical pair: superoxide anion and a semiquinone, which form C4a-hydroperoxide that is capable to decompose into oxidised flavin and H₂O₂.

All flavoproteins are categorized regarding to their reactivity with O₂ and the formed products.

For example, reduced oxidases react very fast with O₂ and give an oxidized enzyme and H₂O₂ as products. On the other hand, reduced monooxygenases react rapidly to form flavin

hydroperoxide. This flavin can oxygenate a substrate or it can eliminate H_2O_2 (Palfey *et al.*, 2011).

Flavoprotein dehydrogenases, however, react much slower with oxygen. Sometimes it can also be much slower than free flavins, just to give a mixture of superoxide anion and H_2O_2 .

Different flavoproteins were studied to determine the basics of acceleration of the reaction with oxygen. There are many suggestions on how enzymes can speed the reaction of reduced flavin with O_2 .

These hypotheses focus on controlling the access of O_2 to the flavin or on stabilizing O_2^- of the radical intermediate. Some studies showed that actually the protein matrix is responsible for guiding oxygen for the reaction in some enzymes.

Moreover, stabilization of the semiquinone-superoxide intermediate helps increasing the reactivity of the flavoproteins. This should consider the polarity of the local environment in which O_2^- is formed (Palfey *et al.*, 2011).

Generally, it was shown that a single mechanism can not be used for explaining oxygen activation in flavoproteins and that several strategies exist in flavoproteins. This can be rationally explained because of the variety of flavoproteins that can react with oxygen.

1.5 Berberine bridge enzyme (BBE)

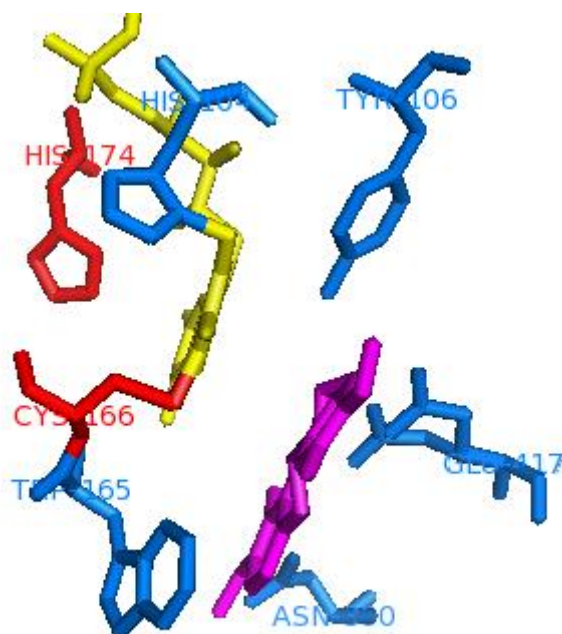


Figure 4: Schematic representation of the structure of active site of BBE in complex with (*S*)-reticuline. The flavin cofactor is shown in yellow with its bicovalent linkage to His104 and Cys166 shown in red. Important active site amino acid residues are drawn in blue. The substrate (*S*)-reticuline is shown in magenta.

1.5.1 General introduction

BBE belongs to the group of flavin-dependent oxidases and can be found in different plant genera like *Berberidaceae* or *Papaveraceae*. It catalyzes the oxidative cyclisation of the *N*-methyl group of (*S*)-reticuline into the C8 carbon atom of (*S*)-scoulerine in bezylisoquinoline alkaloid biosynthesis. So far BBE from *Eschscholzia californica* (Dittrich and Kutchan, 1991), *Papaver somniferum* (Facchini *et al.*, 1996), *Berberis beaniana* (Steffens *et al.*, 1985) and *Thalictrum flavum* (Samanani *et al.*, 2005) were investigated.

As mentioned before, the oxidative cyclisation is responsible for formation of (*S*)-scoulerine (see figure 5). The newly formed product is as precursor in the biosynthesis of

many other alkaloids like protopine and protoberberine alkaloids that are widely spread in *Berberidaceae* and *Papaveraceae* plant families.

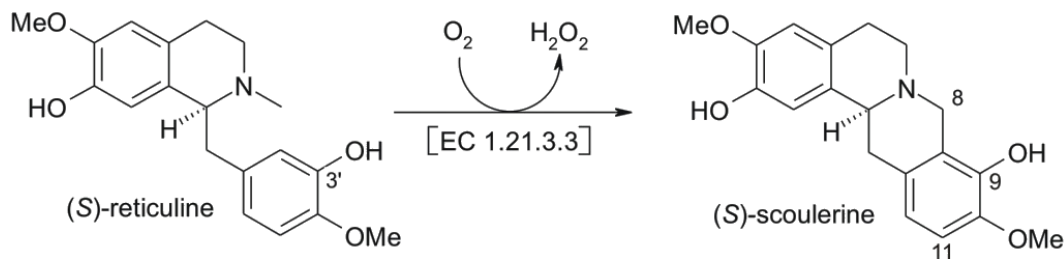


Figure 5: Overall reaction catalysed by BBE (Winkler *et al.*, 2006).

The first isolation of BBE goes back to 1975, when Rink and Böhm reported the partial purification of the enzyme from *Macleaya microcarpa* cell cultures. Later the enzyme was expressed in small amounts in insect cell culture, which enabled a first biochemical characterization and the identification of the covalent cofactor tethering to a histidine residue of the protein (Kutchan and Dittrich, 1995).

The cDNA of BBE from *E. californica* was isolated by Kutchan and coworkers, which allowed a detailed characterisation of the respective enzyme. The isolated cDNA encodes for a protein that consists of 538 amino acids. The first 23 N-terminal amino acids operate as signal peptide for cotranslational transport into the endoplasmatic reticulum (ER). In addition to this targeting sequence, there is a second N-terminal sequence element, which is necessary for targeting the protein into vacuoles.

BBE possesses various sites for posttranslational N-glycosylation. Moreover, BBE has a bicovalently attached cofactor.

Recent studies on different oxidases showed that catalysis requires stabilisation of the transiently formed negative charge at the N(1)-C(2)=O locus of the flavin cofactor (Heuts *et al.*, 2009).

Hence, some positively charged amino acids like arginine or lysine are often positioned in near vicinity to the N1 position of the isoalloxazine ring to stabilize the uptake of the negative charge in the flavin ring system. On the other hand, a histidine residue or helix

dipole can give the positive charge which is important for stabilisation (Wohlfahrt *et al.*, 1999).

In case of BBE this kind of stabilization of the N(1)-C(2)=O locus is not observed. This indicates that stabilisation of the negative charge can be attributed to some other mechanism.

However, although the positive charge is missing in BBE, a tyrosine and a histidine residue are positioned near the N(1)-C(2)=O locus. On this way these two residues can interact directly or via a the C2` hydroxyl group of the ribityl side chain of the flavin. Thus studies were performed to investigate the role of these two residues on BBE. Whereas no specific function could be attributed to the tyrosine residue, the histidine residue His174 showed clear effect on the protein.

His174 was identified as crucial active site residue. It forms a hydrogen bonding network via the hydroxyl group of the C2` atom of the ribityl side chain, which stabilizes negative charge at the N(1)-C(2)=O locus.

Mutagenic analyses revealed more information about the role of bicovalent flavinylation for catalysis and to the proposal of a mechanism for BBE.

In addition to the characterisation of the covalent linkage, a more detailed reaction mechanism is described in figure 6 (Winkler *et al.*, 2008).

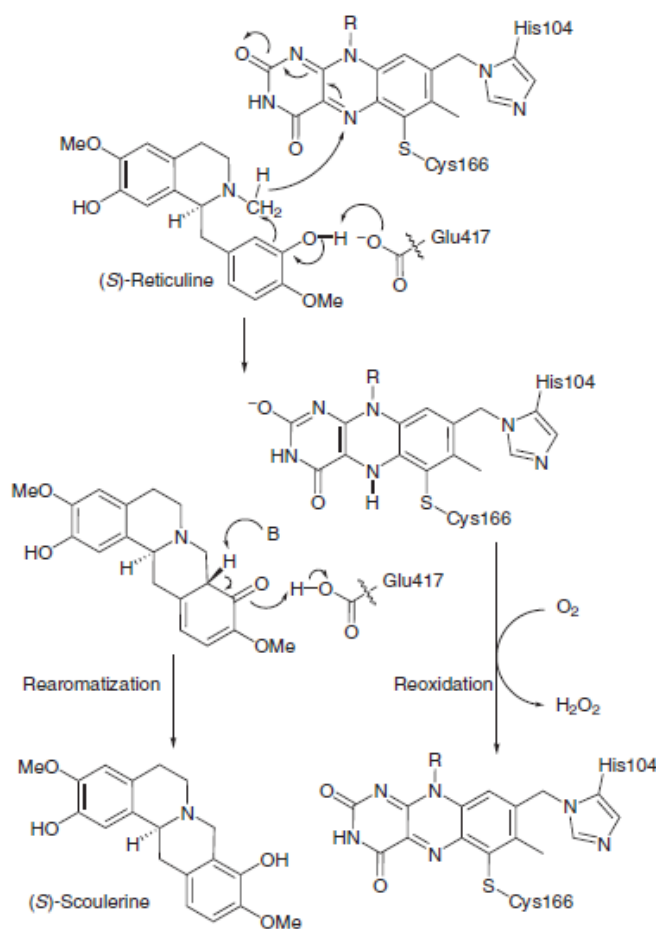


Figure 6: Proposed reaction mechanism for the BBE-catalyzed reaction (Winkler *et al.*, 2008).

Reduction of the cofactor is initiated by deprotonation of C3' OH by Glu417. This increases the nucleophilic behavior of the aromatic ring, thereby allowing carbon-carbon bond formation in a Friedel-Crafts-like alkylation reaction. The formal leaving group, a hydride, is at the same time transformed to the flavin cofactor. Rearomatization of the intermediate substance leads to (S)-scoulerine and might occur spontaneously in solution or could be assisted by another active site base (depicted as B in figure 6). Regeneration of the cofactor is accomplished by reaction with molecular oxygen and generation of hydrogen peroxide (Winkler *et al.*, 2008).

1.5.2 Strategies for BBE expression

Saccharomyces cerevisiae was chosen for first expression experiments and verification of isolated cDNA (Dittrich and Kutchan, 1991). Because of problems with reproducibility, this expression system was not used for large scale production.

Another system described by Kutchan *et al.* (1994) is the use of insect cell cultures. *Spodoptera frugiperda* cells (Sf9) were used as expression host for obtaining larger amounts of protein. These experiments resulted in the production of 4 mg of purified enzyme per liter of cell culture. But nevertheless, there are several drawbacks of insect cell cultures like sensitivity to smallest temperature changes, infections, and shear forces. Difficult handling and time consumption are also negative sites of this system.

Nowadays BBE is expressed in the methylotrophic host *Pichia pastoris*. Usage of this host system enabled the production of sufficient quantities of purified BBE from *E. californica*, allowing a more detailed characterisation of the enzyme (Winkler *et al.*, 2007). Expression in *Pichia* has some major advantages compared to *Saccharomyces*, for example generally higher expression levels, the recognition of signal peptides of various plants, the lack of hyperglycosylation together with the possibility of efficient secretion into the fermentation medium.

1.5.3 Aims of the thesis

Today BBE is a well investigated bicovalently flavinylated oxidase, which is capable of catalyzing a crucial branch-point reaction in benzyloquinoline alkaloid biosynthesis. Thus new studies focus on the identification of BBE-like enzymes in other species. However, there are also new aspects, which can be investigated by performing in-depth studies on BBE. Through exchange of different amino acids in the active site, it is not only possible to change the structure of the enzyme, furthermore also the stability and chemical reactions of the respective variant can be changed.

A general aim of this project was to perform new studies on berberine bridge enzyme by creating a His174Asn variant. This variant was designed for studying the influence of this amino acids on flavin reactivity with oxygen. From sequence alignments it is known that His174 of BBE is strictly conserved among bicovalently linked flavoprotein oxidases and that an asparagine residue is present at the respective position of bicovalently flavinylated dehydrogenases. The central objective of the thesis was to exchange the responsible amino acids to convert BBE wild type oxygenase into dehydrogenase and to express the protein using *Pichia pastoris* as host system to generate enough protein sufficient for detailed biochemical and structural studies.

2 Materials

If not otherwise mentioned all chemicals were purchased from one of the following companies: Sigma-Aldrich (St. Louis, USA), Roth (Karlsruhe, Germany), Fluka (St. Louis, USA) or Merck (Darmstadt, Germany).

For expression in *P. pastoris* special Yeast extract and Bacto Peptone from BD were used. T4 DNA ligase and restriction enzymes were purchased from Fermentas.

2.1 Culture media

LB-medium: 10 g/L tryptone, 5 g/L yeast extract, 5 g/L NaCl

25 µg/mL zeocin was added for *P. pastoris* strains containing pPICZ alpha

LB-medium for agar plates: 15 g/L agar was added to the LB-medium

YPD-medium: 10 g/L BD Bacto yeast extract, 20 g/L BD Bacto peptone, 20 g/L glucose

Glucose was autoclaved separately from other media components and was added after cooling to room temperature.

YPD-medium for agar plates: 15 g/L agar was added to the YPD-Medium

YPG-medium: 10 g/L BD Bacto yeast extract, 20 g/L BD Bacto peptone, 2% glycerol

(20 mL/L)

All media were autoclaved at 121 °C for 20 min. Zeocin was sterilised via filtering and added to the media after cooling to room temperature.

BMD: 200 mL 2M PPB, 100 mL 10x YNB, 50 mL 10x D-Glucose, 2 mL 500x biotin, 650 mL H₂O sterile

BMM10: 20 mL 2M PPB, 10 mL 10x YNB, 5 mL methanol, 0.2 mL 500x biotin, 65 mL H₂O sterile

BMM2: 20 mL 2M PPB, 10 mL 10x YNB, 1 mL methanol, 0.2 mL 500x biotin, 69 mL H₂O sterile

Media components were autoclaved separately and were mixed after sterilization. Biotin was filter-sterilized.

2.2 Buffers and solutions

2.2.1 Buffer and gel for agarose gel electrophoresis

50x TAE-buffer: 2 M Tris/Acetate, 0.05 M EDTA, pH 8.5

1% agarose gel: 1 g agarose per 100 mL TAE-buffer

Table 1: Buffers and solutions for SDS-polyacrylamid gel electrophoresis.

	12.5 % Separating Gel	5 % Stacking Gel
40% acryl amide / 0.8% Bis	3.12 mL	562.5 µL
1.5 mM Tris-HCl, pH 8.8	3.75 mL	---
0.5 mM Tris-HCl, pH 6.8	---	625 µL
20% SDS	50 µL	25 µL
H2O deion.	2.99 mL	3.69 mL
10% ammonium peroxodisulphate	48 µL	25 µL
TEMED	10 µL	5 µL

Staining Solution: 75 mL/L acetic acid, 500 mL/L ethanol, 2.5 g/L Brilliant Blue R

Running Buffer: 15 g/L TRIS, 71 g/L glycine, 2.5 g/L SDS, 1.68 g/L EDTA

Destaining Solution: 75 mL/L acetic acid, 200 mL/L ethanol

2x Sample Buffer: 1 mL Tris-HCl pH 6.8, 400 mg SDS, 300 mg DTT,

20 mg Bromphenol Blue, 2 mL glycerol, 10 mL H₂O

2.2.2 Buffers for western blot

10x TBS (for anti-flavin antibody): 80 g NaCl, 2 g KCl, 30 g Tris Base in 1L water, pH to 8.0 with 1M HCl

10x TBS (for anti-BBE antibody): 80 g NaCl, 30 g Tris Base in 1L water, pH to 8.0 with 1M HCl

TTBS: TBS with 0.05% Tween for BBE-like, and TBS with 0.1% Tween for His174Asn

2.2.3 Buffers for protein purification

Hydrophobic interaction chromatography: 50 mM potassium phosphate buffer, 1 M ammonium sulphate, pH 7.5

Size exclusion chromatography: 150 mM NaCl, 100 mM Tris/HCl, pH 9.0

Ion exchange chromatography: Buffer A (50 mM Tris/HCl, pH 9.0)

Buffer B (50 mM Tris/HCl, 1 M NaCl, pH 9.0)

2.2.4 Other buffers

Activity assay buffer: 1 M Tris/HCl, pH 9.0

Buffer for redox potential determination: 50 mM potassium phosphate buffer, pH 7.0

Buffer for photoreduction: 50 mM potassium phosphate buffer, pH 7.0

Buffer for steady-state kinetics: 0.1 mM Tris/HCl, pH 9.0

2.3 Standards

DNA-Standard: λ -DNA / *Pst* I Marker (Fermentas)

Protein Standard: LMW-Standard (97 kDa, 66 kDa, 45 kDa, 30 kDa, 20 kDa, 14 kDa),
(Amersham Biosciences)

2.4 Kits

Mutagenesis Kit: QuikChange[®] XL Site-Directed Mutagenesis Kit (Stratagene)

Plasmid Purification: Nucleospin Plasmid Quick Pure (Macherey-Nagel)

NucleoBond[®] PC100 (Macherey-Nagel)

2.5 *Pichia* strains

Table 2: *Pichia* strains used in this master thesis.

Strain	Application
<i>P.pastoris</i> KM71H	expression strain
<i>P.pastoris</i> KM71H [pPICK-PDI]	expression strain (coexpressing the protein disulfide isomerase of <i>S. cerevisiae</i> for facilitated protein folding)

2.6 Primers

Forward primer: 5'-ccgttggtactgggggtaatattagtgggtgg-3'

Reverse primer: 5'-ccaccaccactaatattacccccagtaccaacgg-3'

2.7 Vectors

Table 3: Vectors used in this master thesis.

Vector	Application
pPICZalpha	Expression in <i>P.pastoris</i>

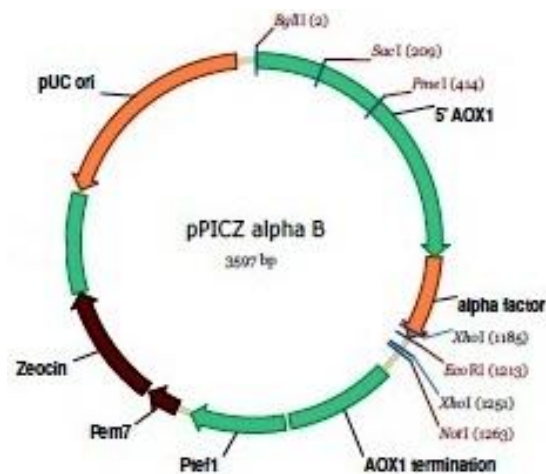


Figure 7: pPICZalpha vector used in this master thesis.

2.8 Equipment

PCR devices	2720 Thermal Cycler (Applied Biosystems) Primus 25 advanced (peqlab)
DNA electrophoresis equipment	Sub-Cell [®] GT Agarose Gel Electrophoresis System (BIO-RAD)
Agarose gel documentation system	Gel Doc 200 (BIO-RAD)
Electrophoresis power supply	PowerPac [™] 300 (BIO-RAD)
Protein electrophoresis equipment	Mini-PROTEAN [®] 3 Cell (BIO-RAD)
Fermenter	Infors HT Multitron Standard (Infors)
Centrifuges	Heraeus Fresco [™] 17 Centrifuge (Heraeus) Heraeus Labofuge 400R (Heraeus) Sorvall [®] RC-5B Plus Du Pont (Thermo scientific) Sorvall [®] RC-6 Plus Du Pont (Thermo scientific)
Others	ISS110 SpeedVac [®] System (ThermoSavant) Centriprep [®] 10 kDa MWCO (Millipore) Eppendorf Thermomixer comfort (Eppendorf) Gene Pulser [®] II electroporator (BIO RAD) Fermenter BBI Biostat CT5-2 (Sartorius)

3 Methods

3.1 Standard methods

All standard methods like sterile working techniques or sterilisation of different media components were performed according to standard protocols.

3.2 Plasmid isolation

For plasmid isolation ONCs were prepared in 50 mL LB-media and incubated over night at 37 °C. Following day plasmids were isolated using the plasmid purification kit from Macherey-Nagel.

For cultivation on plates the cultures were streaked on fresh LB-plates and incubated over night at 37 °C. Again DNA was isolated from the fresh culture using the plasmid purification kit from Macherey-Nagel.

3.3 Restriction

Vectors and inserts were treated with restriction enzymes to generate sticky ends for religation. After restriction, the desired DNA fragments were purified from an agarose gel using gel extraction according to standard protocols.

Xho I and *Not* I were used for treating both vector and insert.

3.4 Ligation

In most cases ligation was done in two hours at 22 °C. For better ligation efficiencies the reactions were performed over night at 16 °C. For a typical ligation reaction 100 ng of vector were mixed with a 4-fold excess of insert and treated with 1 µL T4 DNA ligase in T4 DNA buffer. The total reaction volume was 20 µL.

3.5 Transformation into *P. pastoris*

Approximately 1-5 µg of linearized plasmid DNA was mixed with 40 µL of competent cells and incubated on ice for five minutes. Samples were electroporated using the following parameters: cuvette gap, 2.0 mm; charging voltage, 1500 V; resistance, 200 Ω; capacitance, 25 µF. Immediately after electroporation samples were resuspended in 1.0 mL recovery medium and incubated in a 30 °C shaker for 2 hours. After that the cells were streaked on plates containing increasing concentrations of zeocin and incubated at 30 °C until single colonies were formed.

3.6 Site directed mutagenesis

Mutagenesis was performed following the instructions of the QuikChange[®] XL Site-directed Mutagenesis kit (Stratagene). The expression vector pPICZα BBE-ER was used as template for the polymerase chain reaction. Replacement of His174 with Asn was accomplished by using 5'-ccgttggtactgggggtaaatattagtggtggtgg-3' as sense and the complementary antisense primer. The underlined nucleotides represent the mutated codon. Introduction of the desired mutation was verified by sequencing.

3.6.1 Expression in 96-deep-well plates

Every position of the deep-well plate containing 250 µL BMD medium was inoculated with a single expression colony. The plates were incubated at 28 °C and 320 rpm for 2 days for

biomass production. 72 hours after inoculation protein expression was induced by the addition of 250 µL of BMM2 medium to all positions of the deep well plate. Further induction was performed every 12 hours by addition of 50 µL of BMM10 medium.

After 96 hours cells were harvested by centrifugation at 4000 rpm for 15 minutes and the supernatant was used for Dot-Blot analysis (Weis *et al.*).

3.6.2 Expression in 300 mL shake flasks

300 mL shake flasks containing 50 mL BMD-medium were inoculated with a single expression colony. The culture was incubated for two days at 28 °C and 150 rpm. Induction was started after 72 hours by the addition of 5 mL BMM10 medium. Further addition of methanol was performed after 12, 24, 48 and 72 hours by adding 50 µL of pure methanol. The cells were harvested after 96 hours by centrifugation at 4600 rpm for 15 minutes.

3.6.3 Expression in 2L baffled flasks

This method is an optimisation of the protocol for expression in 300 mL shake flasks. Precultures were started in 50 mL of YPG containing 2% glycerol and were used to inoculate main cultures to a starting OD of 1. The fresh inoculum was cleared from residual glycerol. Therefore, precultures were harvested by centrifugation at 3500 rpm for 5 minutes, the cell pellet was dissolved in minimal media with methanol to start the expression.

Samples were taken after 12, 24, 36, 48, 60 and 72 hours always before new induction with methanol. Samples were analysed using Western blots technique to determine the expression level at various time points of expression.

3.7 Dot-Blot

For blotting a nitrocellulose membrane was used. The membrane was soaked in 1x TBS buffer and then applied to the apparatus. Buffer was pulled through the membrane by using a vacuum.

This was followed by loading 200 µL of the supernatant, after 10 minutes incubation on room temperature a vacuum was applied and the solution was pulled through the membrane. Afterwards the membrane was washed with 200 µL 1x TTBS buffer. Using this technique soluble proteins were transferred to the nitrocellulose membrane.

For His174Asn variant the membrane was blocked with 13% milk powder in TTBS for one hour and then repeatedly washed with TTBS. Thereafter, the membrane was incubated with the solution of the first antibody (anti-BBE) over night at 4 °C.

After incubation with the first antibody the membrane was again repeatedly washed with TTBS and then incubated with the secondary antibody (anti-rabbit IgG-POD). After one hour of incubation the membrane was repeatedly washed with TTBS buffer.

For detection SuperSignal[®] West Pico Chemiluminescent Substrate from Thermo scientific was used.

3.8 Sodium dodecyl sulphate-polyacrylamide gel electrophoresis

SDS-PAGE (sodium dodecyl sulphate-polyacrylamide gel electrophoresis) was used to control the expression level of the desired proteins and to estimate the concentration and purity of expressed protein.

Gels consisting of a 12.5% separating gel and a 5% stacking gel were used to separate the proteins according to their molecular weight. Samples were prepared by mixing the protein solutions 1:1 with 2x sample buffer and heating to 95 °C for 10 minutes. All samples and the LMW standard were loaded onto the gel and electrophoresis was started at 120 V for concentrating the proteins in the stacking gel. Subsequently voltage was increased to 160 V for separating the proteins in the separating gel. Visualization of all protein bands was achieved by staining the separating gel with Coomassie Brilliant Blue R for 10 minutes and destaining it with destaining solution. Molecular weight of the proteins was estimated by comparison with known bands of the Low Molecular Weight Standard (Amersham Biosciences).

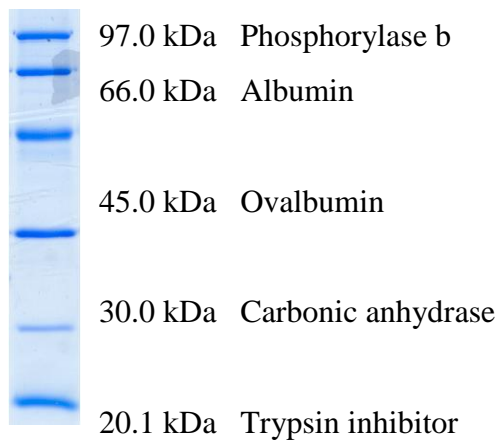


Figure 8: LMW standard for SDS-gels.

3.9 Western Blot

Western Blot technique was used for detecting heterologously expressed protein in expression supernatants. Therefore, samples were concentrated using TCA precipitation and were applied to SDS-PAGE. Then all proteins were transferred to nitrocellulose membranes using a standard protocol. The membranes were blocked with 13% milk powder and incubated with primary antibody (anti-BBE) over night at 4 °C. After 12 hours the membranes were washed with TTBS and incubated for one hour with secondary antibody (anti-rabbit IgG-POD).

Detection was done as described for the Dot-Blot experiment (chapter 3.7).

3.9.1 Colony PCR

Colony PCR was used to amplify DNA fragments directly from single colonies. Using this method it was possible to determine the presence of the expression cassette in the genome of *P. pastoris*. Therefore, some cell material was taken from the agar plate, transferred into the PCR tube and mixed with 50 µL of zymolyase solution (Amsbio). Thereby cell walls were opened and after heating to 92 °C for 5 minutes this solution was used directly as template for the PCR reaction.

Another protocol used for colony PCR consisted of taking a single colony from the agar plate, resuspending it in 100 µL sterile water and heating to 95 °C for 5 minutes.

Afterwards cell fragments were removed by centrifugation. As template 10 μ L of the supernatant was used for 50 μ L of PCR reaction.

Either Phusion polymerase or GoTaq polymerase were used for colony PCR. The program used for colony PCR is listed below.

Table 4: Program used for Colony PCR.

Temperature	Time (seconds)	Cycles
98 °C	30	} 30
98 °C	10	
45 °C	30	
72 °C	30-60 /kb	
72 °C	10 minutes	
4 °C	∞	

3.9.2 Large-scale expression

Large scale expression of BBE was carried out in a BBI CT fermenter (Sartorius) with a digital control unit. Cultivation was conducted with a glycerol batch phase followed by a glycerol-fed batch. After formation of enough biomass, protein production was initiated by addition of methanol. The different stages of fermentation are described in *Pichia Fermentation Process Guidelines* (Invitrogen, Schrittwieser *et al.*, 2011). After 96-h methanol induction, the fermentation was stopped and the cells were separated from the medium by centrifugation at 4000 rpm for 30 minutes.

3.10 Protein purification

The resulting supernatant was then loaded onto a XK50/20 phenyl-Sepharose 6 FF column, which was equilibrated with 20 mM potassium phosphate buffer (pH 7.5) containing 1 M ammonium sulphate. After complete loading and washing with equilibration buffer, BBE was eluted from the column using a gradient from 0 to 100% of 20% ethanol.

BBE containing fractions were determined with activity assay, pooled and concentrated using the Centriprep system from Amicon.

Aliquots of 2 mL from the resulting strong green solution from the HIC column were then loaded onto a HiLoad™ 16/60 Superdex™ 75 prep grade (Amersham Biosciences) gel-filtration column equilibrated with the storage buffer of BBE (150 mM NaCl, 50 mM Tris/HCl, pH 9.0). Fractions were eluted at a flow rate of 1 ml/min. Eluted fractions were analysed by SDS-PAGE and activity assays, BBE containing fractions were pooled and again concentrated by ultrafiltration. In case of His174Asn variant, a further step of purification using ion exchange chromatography was necessary for obtaining highly pure protein.

In a final step aliquots of the concentrated protein from the previous purification step were loaded on a MonoQ column equilibrated with buffer A (50 mM Tris/HCl, pH 9.0). Fractions were eluted at a flow rate of 0.7 mL/min using a gradient to 30% buffer B (50 mM Tris/HCl, 1 M NaCl, pH 9.0) in 30 minutes and finally 100% buffer B in 15 minutes. The collected fractions were then pooled and concentrated by ultrafiltration. Small aliquots of the purified protein sample were flash-frozen to -70 °C.

3.11 Activity assays

BBE activity was determined by monitoring the conversion of (*S*)-reticuline to (*S*)-scoulerine (Winkler et al., 2006). Reaction mixtures consisted of 4 µL of sample, 4 µL of 10 mM (rac)-reticuline and 19 µL of activity buffer (1 M Tris/HCl, pH 9.0) and were incubated at 37 °C for 10 min. For visualization of the conversion the reaction mixtures were separated using thin layer chromatography with CH₂Cl₂/MeOH/NH₃ (90/9/1) as mobile phase and authentic standards for substrate and product as reference.

3.12 Anaerobic photoreduction

For photoreduction of BBE 1 mL of reaction mixture containing 113.6 µM of His174Asn variant, 0.02 M EDTA and catalytic amounts of 5-deazariboflavin in 50 mM potassium phosphate buffer, pH 7.5 was prepared. This mixture was rendered anoxic by placing it in an O₂-free atmosphere in a glowe box from Belle Technology and then keeping it in

special quartz cuvettes. Photoirradiation was then carried out by illuminating the sample with a conventional slide projector and spectra showing the progress of reduction were monitored.

3.13 Steady-state kinetic analysis

For determining steady-state turnover rates, high performance liquid chromatography (HPLC) analysis was applied. For this experiment, a reaction mixture consisting of 14.2 μ M His174Asn variant, 6 μ M (*S*)-reticuline and 457.5 μ L 0.1 mM Tris/HCl pH 9.0 was incubated at 37 °C. Conversion of (*S*)-reticuline to (*S*)-scoulerine was then stopped at different time points by the addition of isopropanol containing 50% TFA mixed 1:1 with Tris/HCl buffer to pH of 1.24. The formation of (*S*)-scoulerine was followed by HPLC.

3.14 Determination of redox potential

Determination of the redox potential of the flavin cofactor was carried out using the dye-equilibration method with the xanthine/xanthine oxidase electron delivering system. Concentrations of protein and redox indicator were chosen so that the absorbance changes at the wavelength important for interpretation of the data were in almost the same absorbance range. Reactions were carried out in 50 mM potassium phosphate buffer, pH 7.0, at 25 °C containing 0.005 mM benzylviologen as mediator, 0.3 mM xanthine, and 0.0095 μ M xanthine oxidase. A typical reduction lasted for one hour in order to ensure equilibration between dye and protein. For maintaining anaerobic conditions, the reduction was carried out in a stopped-flow device (SF-61DX2, Hi-Tech) positioned in an anaerobic glove box. Spectra during the course of reduction were recorded with a KinetaScanT diode array detector (MG-6560) from Hi-Tech. Redox potentials were calculated by plotting $\log(\text{ox/red})$ of dye against $\log(\text{ox/red})$ of the flavin cofactor (Minnaert, 1965).

3.15 Crystallization

Different crystallization methods were used in order to produce diffracting crystals for structure determination. Crystals were grown using the sitting drop method . For this, drops of 1 μL of enzyme solution (~ 33 mg/mL in 50 mM Tris, 150 mM NaCl, pH 9.0) was mixed with 1 μL of reservoir solution (0.2 M MgCl_2 and 30% (w/v) polyethylene glycol 4000 in 0.1 M Tris/HCl, pH 8.5) and equilibrated for 2 hours prior to streak seeding.

Moreover, micro batch experiments using the Index Screen conditions from Hampton were performed. Here the solutions (conditions from Index Screen Hampton research) were directly mixed with pure protein solution in micro batch, covered with oil and incubated at 20 $^\circ\text{C}$.

Formation of protein crystals was observed regularly.

4 Results

4.1 Cloning, expression and purification

4.1.1 Site-directed mutagenesis

Site-directed mutagenesis with a modified two step protocol was successfully used to generate the expression plasmid for the BBE His174Asn variant. The resulting construct [pPICZalpha-BBE His174Asn] was transformed into *E. coli* XL 10 Gold cells. Transformation was successful and isolated plasmid DNA was linearised for transformation in *P. pastoris*. Transformation in *P. pastoris* was done according to the protocol described in chapter 3: Methods.

A representative gel showing the PCR product from mutagenesis PCR is depicted in figure 9.

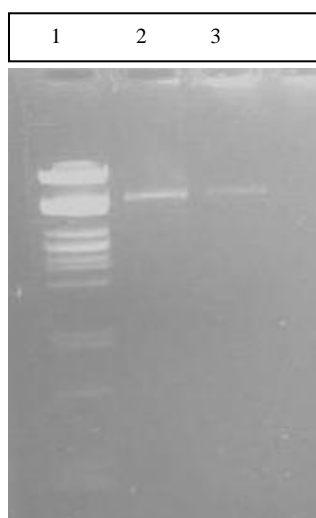


Figure 9: Control gel after mutagenesis PCR; Lane 1: λ -DNA standard digested with *Pst* I (from Fermentas), Lanes 2 and 3: PCR product.

4.1.2 Screening

Screening was carried out for identifying good expression strains with stable and high protein expression. Single colonies were chosen to inoculate 96-well plates and expression was performed as described in chapter 3: Methods.

BBE His174Asn was expressed using pPICZalpha expression kit. Thus, heterologously expressed protein was supposed to be secreted into the medium.

After an induction period of 96 hours the cells were harvested and the supernatant was analysed for BBE activity. All screens were performed in 96-well plates and the best transformants were selected for further expression in shake flasks and in a 7 L bioreactor. Dot blot experiments were used to identify applicable expression strains. The best expression strains identified in three rounds of screening were WT G8 and PDI F3. WT G8 is an expression strain, where the expression plasmid was transformed into *P. pastoris* KM71H. For PDI F3, a strain coexpressing the protein disulfide isomerase from *S. cerevisiae* was used. The variants were taken by comparing the strength of signal with BBE W165F when anti-BBE antibody was used for protein detection.

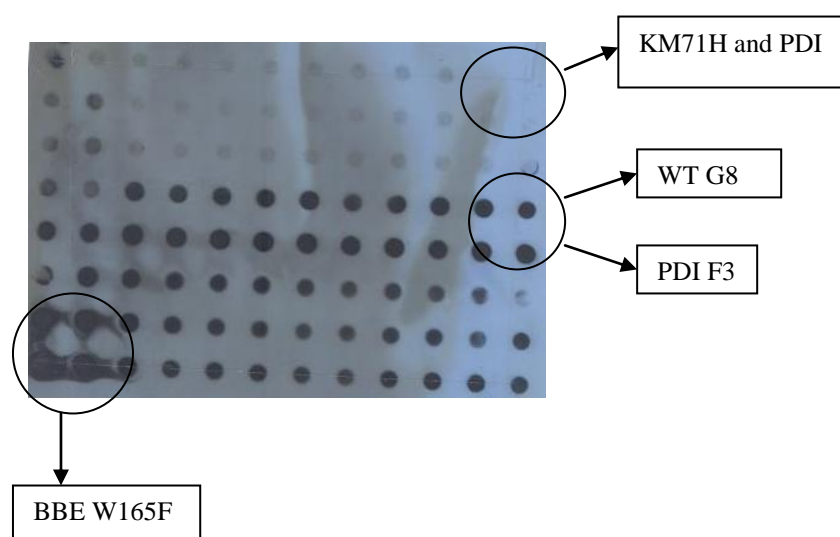


Figure 10: Dot Blot for H174N. BBE W165F was used as positive control, whereas *P. Pastoris* KM71H and the strain coexpressing PDI were used as negative controls. Dot blot was performed using the anti-BBE antibody and a second antibody coupled to a peroxidase for detection.

4.1.3 Small-scale expression

Small-scale expression was performed using first 300 mL shake flasks. In these experiments no BBE activity was detected in supernatants after expression. Consecutively, the expression was done in 2 L baffled flasks in an optimized YPG medium. Again the expression was not satisfactory although SDS gels showed the formation of a protein with the approximate molecular weight of 66 kDa in the course of induction. Those bands were cut out for MALDI-TOF analysis. Unfortunately, the results did not show expressed BBE protein.

A test purification step via hydrophobic interaction chromatography showed that the amount of expressed protein was not sufficient for the two-step purification protocol as described for wild type BBE.

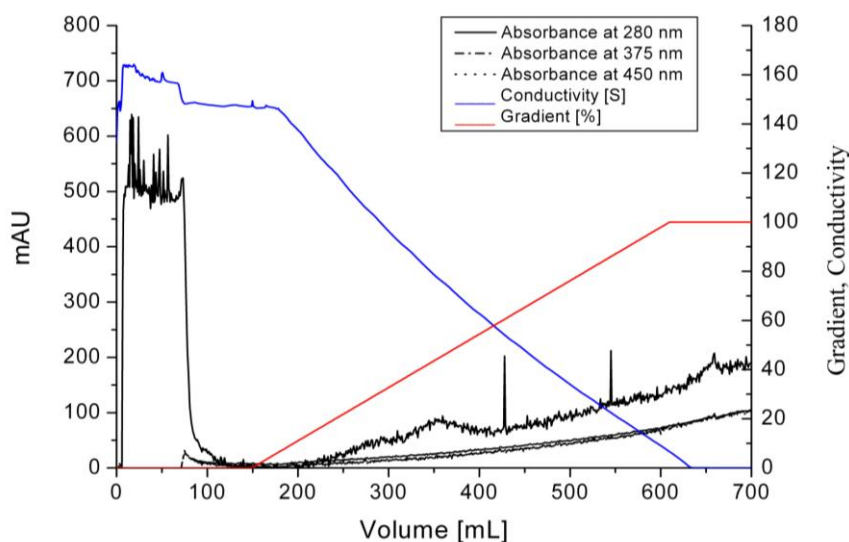


Figure 11: Purification of H174N PDI F3 via hydrophobic interaction chromatography after expression in shake flasks. The blue line shows the conductivity, whereas the red line represents the applied gradient. The solid black line shows absorption at 280 nm, and the two dotted lines show absorbance at 375 and 450 nm, respectively.

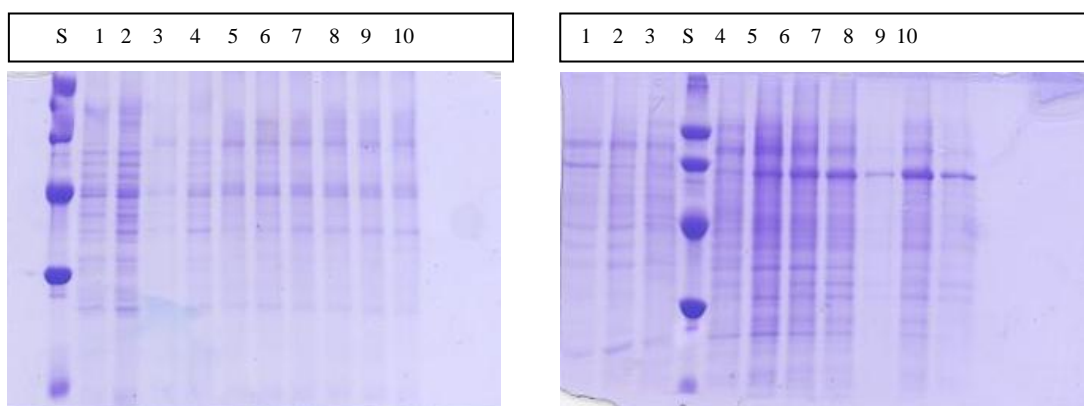


Figure 12: Left: SDS Gel of the course of expression of WT G8; Lane S: LMW protein standard, Lane 1: secreted protein fraction before induction, Lanes 2-10: secreted protein fractions taken 12 h, 24 h, 36 h, 48 h, 60 h, 72 h, 84 h, 96 h, and 108 h after first induction.

Figure 13: Right: SDS Gel of the course of expression of PDI F3; Lane S: LMW protein standard, Lane 1: secreted protein fraction before induction, Lanes 2-10: secreted protein fractions taken 12 h, 24 h, 36 h, 48 h, 60 h, 72 h, 84 h, 96 h, and 108 h after first induction.

Due to severe problems with reproducibility of expression yields it was necessary to switch to bioreactor fermentation where a better control of critical parameters during methanol induction (dissolved oxygen level, constant methanol supply, pH adjustment, and temperature) can be achieved.

4.1.4 Bioreactor fermentation

Heterologous expression of BBE His174Asn was successfully achieved using a 7 L bioreactor with process control. Fermentation was performed according to the manual described in chapter 3: Methods with pH 6.0. Biomass was produced in a batch reactor followed by a fed-batch phase using glycerol as carbon source. After reaching necessary cell densities, heterologous protein expression was induced by the addition of methanol.

After 96 hours of induction, cells were harvested by centrifugation. The supernatant was supplied with 1 M ammonium sulphate and loaded onto a XK 50/20 phenylsepharose 6 FF (high substitution) column and purified as described in chapters 2 and 3: Materials and Methods.

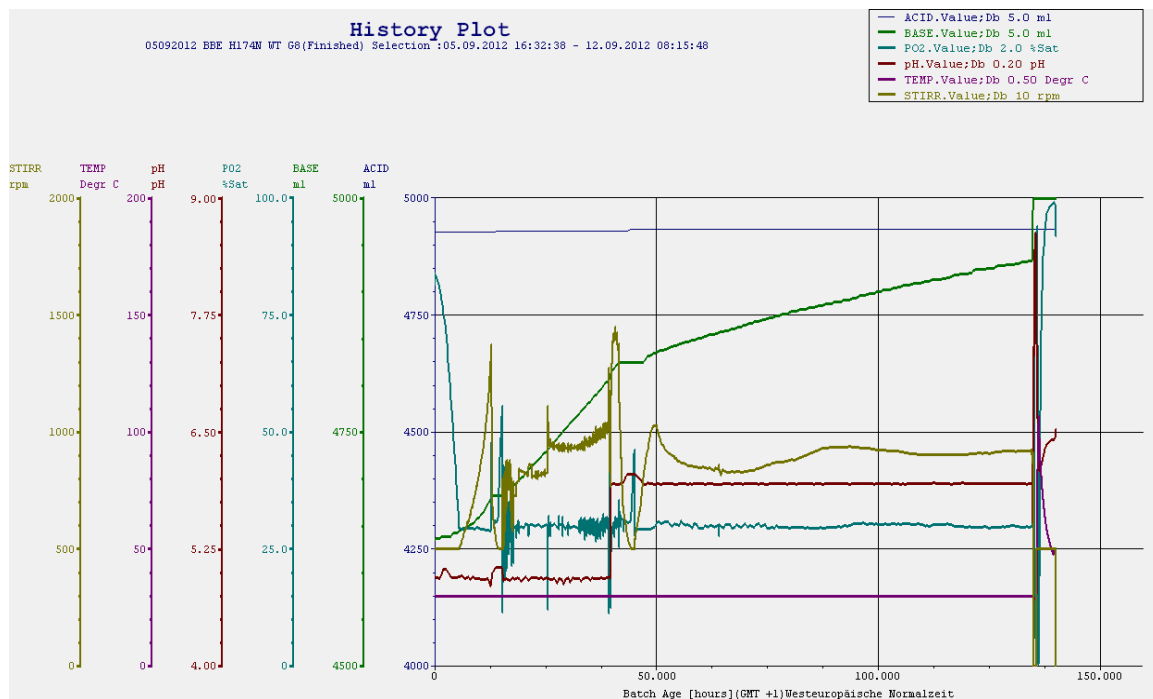


Figure 14: Fermentation of *P. pastoris* KM71H [pPICZalpha-BBE His174Asn]. Important process parameters as pH-value, oxygen saturation, stir speed, temperature, and addition of base and acid are depicted in the diagram. Yellow line represents stir speed, whereas violet line represents the reactor temperature. pH value is shown in red line, followed with cyan line which represents oxygen saturation (pO₂). Addition of base is shown with green line.

Figure 14 shows the large-scale expression of BBE His174Asn in *P. pastoris* KM71H. Important process parameters like pH value, oxygen saturation (pO₂), stir speed, addition of base and acid, and airflow (oxygenation) are shown in the diagram. During biomass production the pH value was adjusted to pH 5.0, during methanol induction pH was increased to 6.0. The diagram shows the expression from the initial batch and fed-batch phase for biomass production, continued with methanol feeding. Stir rate was automatically controlled to set the dissolved oxygen concentration to 30% during the whole course of fermentation.

4.1.5 Protein purification

After centrifugation, the supernatant supplied with 1 M ammonium sulphate was loaded on a HIC column and eluted using a linear gradient against 20% ethanol. Fractions with absorbance at 450 nm (indicative for the presence of a flavin cofactor) were analysed via SDS PAGE and activity assays (see figures 16 and 17). Fractions showing BBE activity were pooled and concentrated for a further purification step. After this first purification step fractions with BBE activity also contained large amounts of a green impurity, which increased the absorbance at 450 nm.

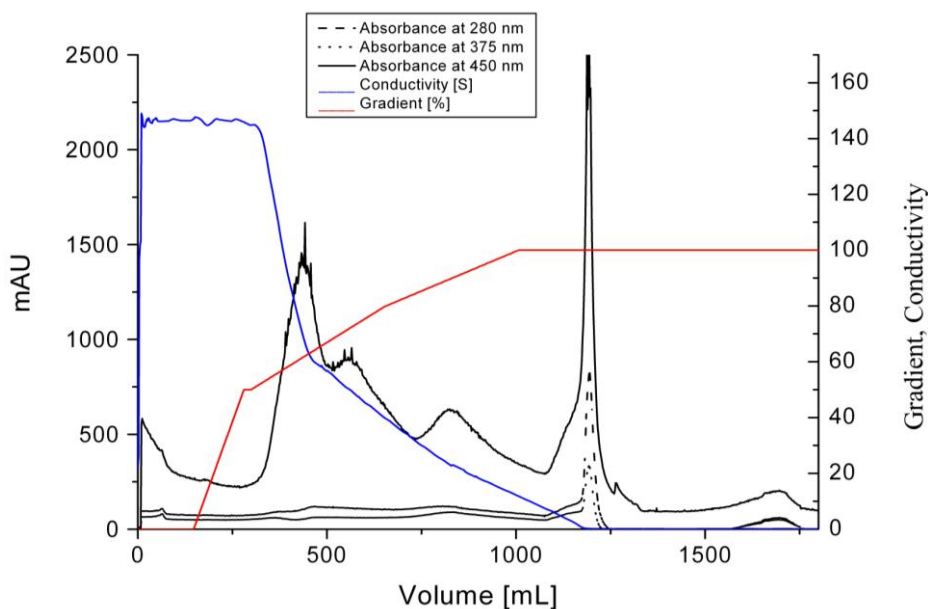


Figure 15: Purification of BBE His174Asn using hydrophobic interaction chromatography. *Black solid line* shows the absorbance at 280 nm. *Two dotted lines* show the absorbance at 375 and 450 nm, respectively.

As expected, the large scale expression of His174Asn resulted in formation of larger quantities of secreted protein as compared to the small scale expression in shake flasks. Protein yields were sufficient for performing the two-step protocol established for BBE wild type.

Fractions after purification via HIC column were analysed via SDS PAGE and activity assay. Only those fractions that showed activity and 66 kDa protein on SDS PAGE were pooled and concentrated for further purification.



Figure 16: Activity assay after purification via HIC column. Lane 1: negative control; Lane 12: positive control; Lanes 2-11: protein fractions of BBE His174Asn after purification via HIC column.

As obvious from the SDS-gel, fractions containing 66 kDa protein were concentrated and applied to a gel filtration column for removing further impurities.

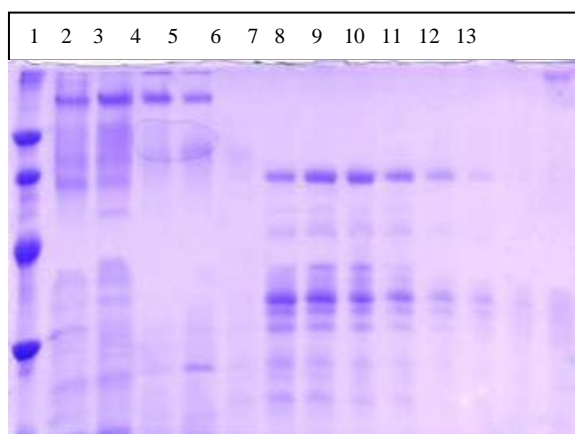


Figure 17: SDS PAGE of fractions from purification of His174Asn via HIC. Lane 1: LMW Standard, Lanes 2-13: Protein fractions, Lanes 6-11: Fractions where 66 kDa protein was found.

With the two-step protocol it was possible to remove impurities and yield 115 mg of BBE His174Asn from one 7 L bioreactor.

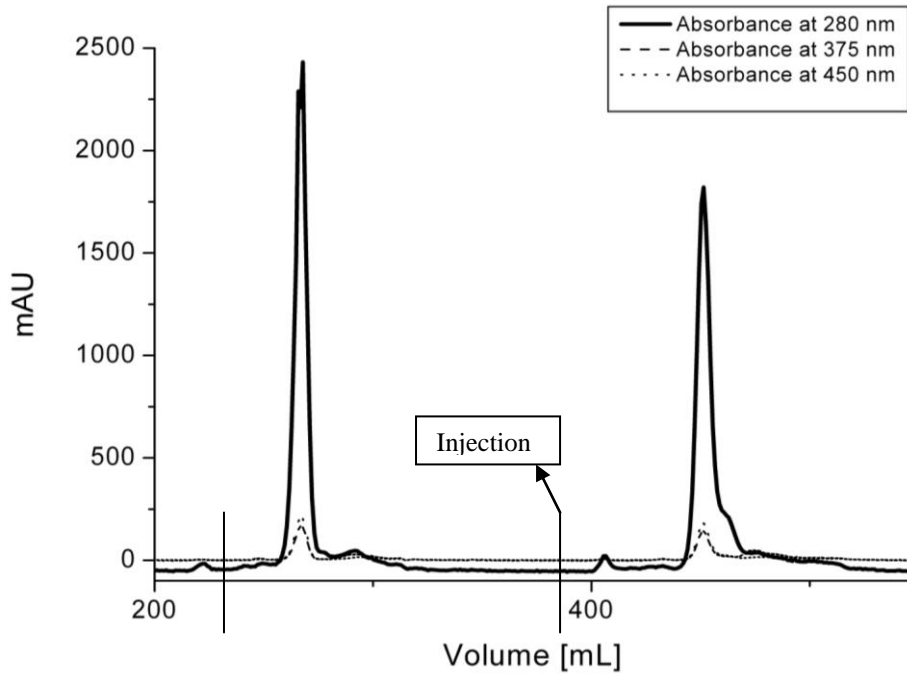


Figure 18: Size exclusion chromatography as second step for the purification of BBE His174Asn. Injection timepoints are marked with straight solid lines. The peaks represent run 1 and run 2, respectively.

Again all runs were analysed with SDS-PAGE and activity assays.

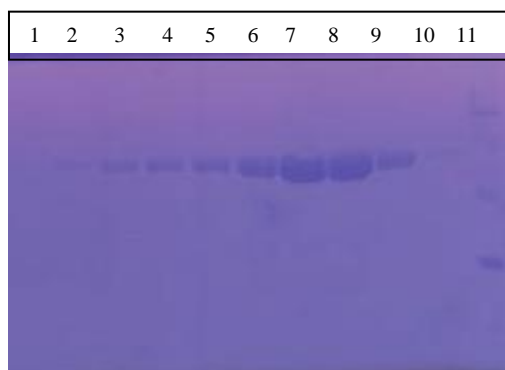


Figure 19: Representative SDS-gel of fractions after size exclusion chromatography. Bands on the gel represent 66 kDa protein.

Fractions containing BBE were pooled and concentrated. When necessary these fractions were then subjected to a final purification step using an anionic exchange column for removing the remaining green impurities. However, anion exchange using MonoQ-column was always sufficient for yielding satisfactory pure protein.

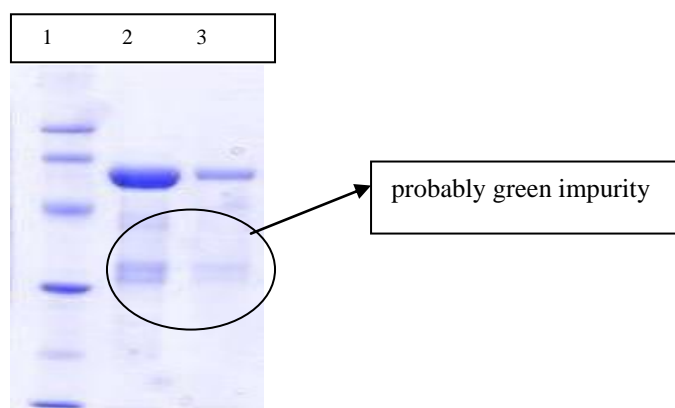


Figure 20: Concentrated fractions after gel filtration. From left to right: Lane 1: LMW protein standards, Lanes 2 and 3: concentrated protein fractions from run 1 and run 2, respectively.

As obvious from figure 20, the protein fractions after gel filtration still were contaminated with other proteins and required a further purification step. For yielding highly pure protein for crystallization experiments, the fractions were finally applied onto a MonoQ column and eluted in a linear gradient with increasing ionic strength as described in chapter 3: Methods.

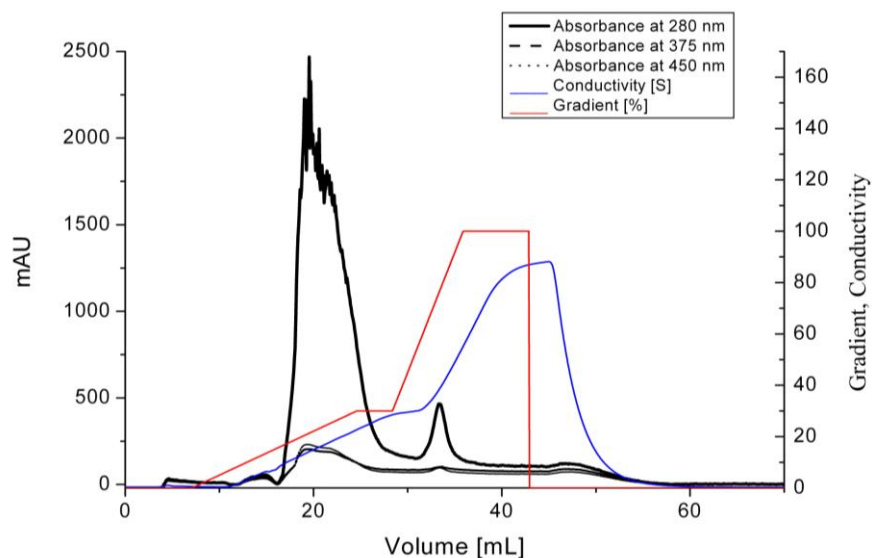


Figure 21: Final purification step via ion exchange chromatography. *Black solid line* represents absorbance at 280 nm, followed by two *dotted lines* which represent absorbance at 375 and 450 nm. The *blue solid line* represents conductivity, the *red solid line* the linear gradient with increasing ionic strength.

Concentration of the pure protein was determined by measuring the absorbance of the oxidized flavin cofactor at 450 nm. Full absorbance spectra were recorded to monitor protein purity. Contaminations with the green non-identified impurity were observable as absorption maximum at 610 nm.

Table 5: Photometric determination of protein concentration.

Protein fraction	Concentration [μ M]	Total amount [mL]
Fraction 1	568	3
Fraction 2-highly pure	1535.3	1

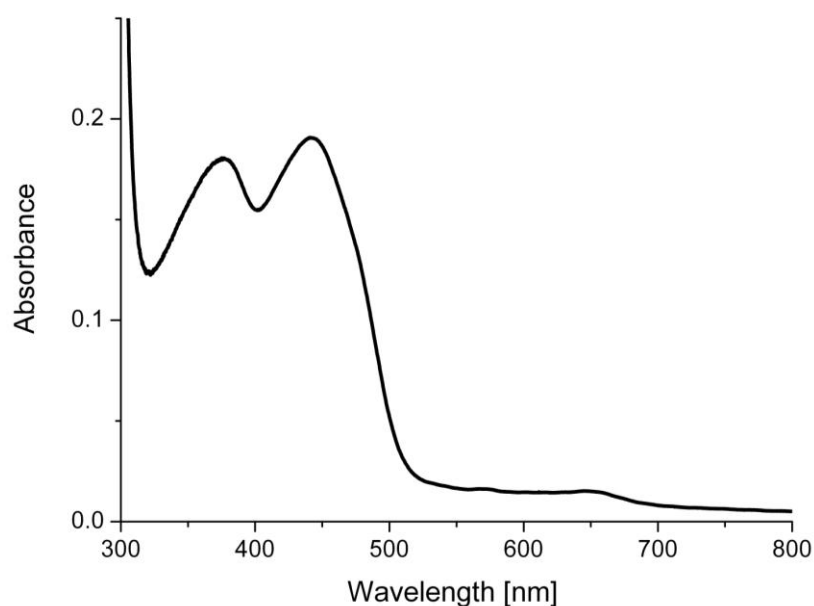


Figure 22: Absorbance spectrum of BBE His174Asn.

4.2 Protein characterisation

4.2.1 Anaerobic photoreduction

Reduction of BBE His174Asn by light was performed in the presence of EDTA and 5-deazariboflavin followed by reoxidation upon admission to oxygen. Light illumination led to formation of a thio-flavin product as characterized by the broad absorption around 800 nm, which was observable after reoxidation (see figure 23).

This experiment can be used to discriminate between single electron transfer and two electron transfer to the flavin cofactor. Figure 23 shows the course of flavin reduction upon irradiation with light. The protein sample was subjected to irradiation with light and spectra were recorded after certain time periods. After full photoreduction (see figure 24), the anaerobic cuvette was opened and incubated for two minutes to allow completely reoxidation of the flavin cofactor.

Upon photoreduction BBE His174Asn showed a behaviour, which was comparable to wild type BBE. During the course of photoreduction the formation of a red anionic radical was observed, which disappeared again and complete photoreduction resulted in a typical spectrum of a reduced flavin cofactor. As we can see from figure 23, there are different isosbestic points observable during photoreduction. One isosbestic point is between oxidised flavin and red radical, followed with another one between red radical and reduced flavin. The last one is between reduced flavin and thio-flavin product.

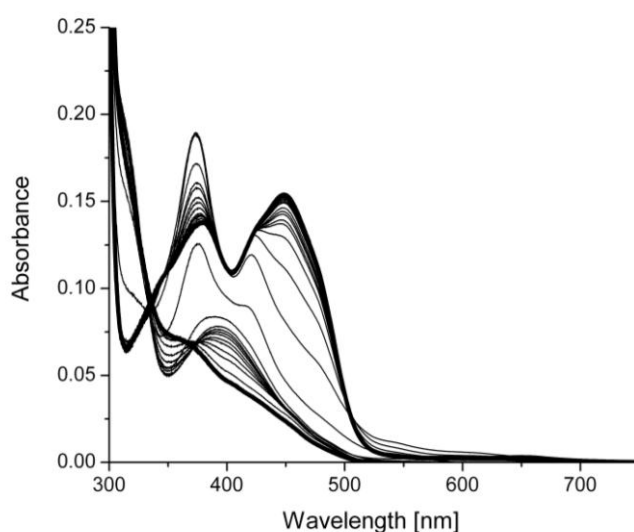


Figure 23: Selected spectra of the complete photoreduction of BBE His174Asn. *Solid lines*, spectra recorded before illumination with light, during photoreduction and spectrum of the fully reduced species.

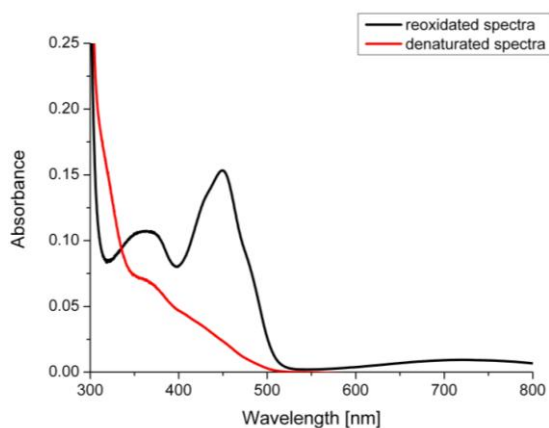


Figure 24: Reoxidation upon admission of oxygen. *Red solid line*, fully reduced spectrum. *Black solid line*, flavin cofactor 2 min after admission of oxygen.

Additionally, another photoreduction experiments were performed, but protein was not fully reduced. This was done to observe the formation of the thio-flavin product which forms after full reduction of protein.

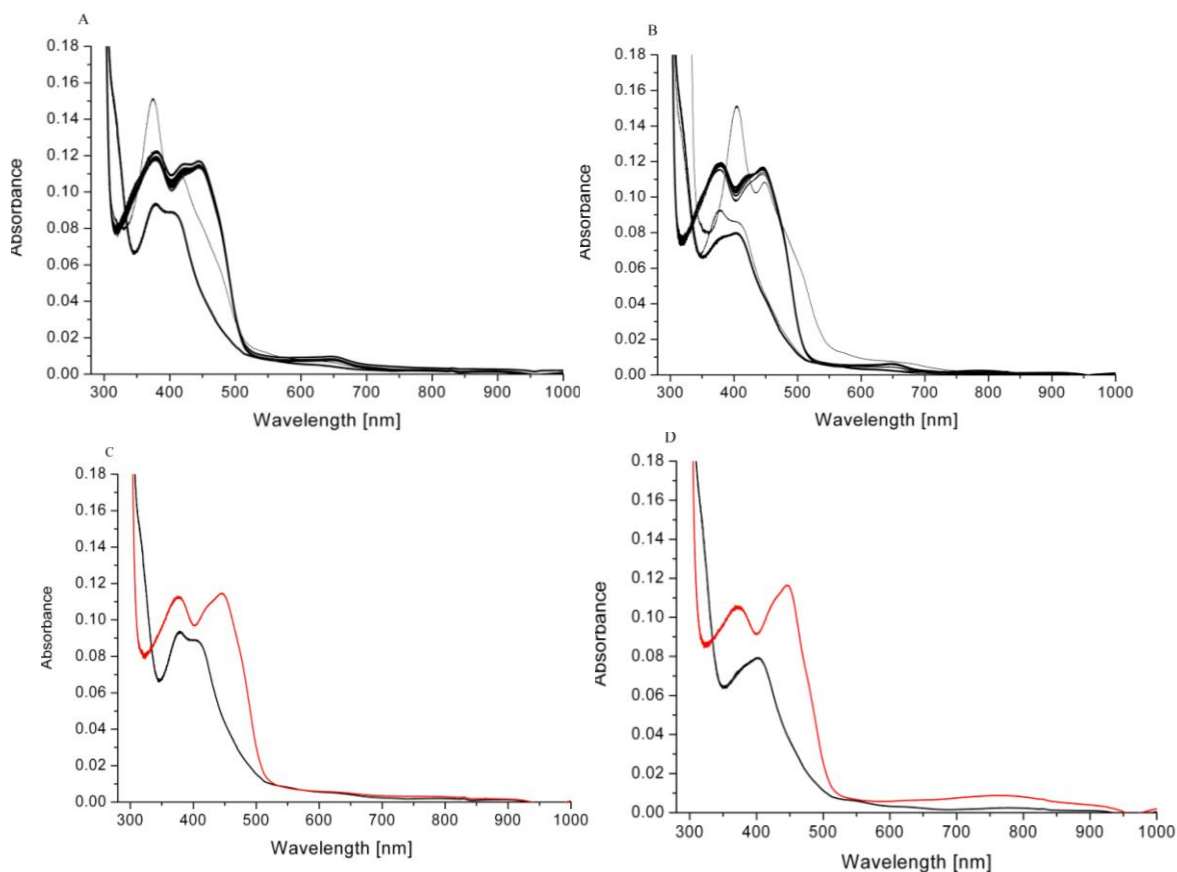


Figure 25: Diagrams A and B represent unfinished photoreduction of BBE His174Asn, whereas diagram B represents photoreduction with one more step. Diagrams C and D represent the fully reoxidation of flavin cofactor upon admission of oxygen. Diagram D shows the formation of thio-flavin product after photoreduction (diagram B) was performed with one more irradiation step.

As represented on figure 25, one further irradiation step in photoreduction of BBE His174Asn (diagram B) leads to formation of thio-flavin product during reoxidation upon admission of oxygen (diagram D).

4.2.2 Steady-state kinetic analysis

The turnover rate was determined under optimized conditions which were already used for the determination of the k_{cat} -value of wild type BBE, His174Ala, and the Trp165Phe variant (Winkler *et al.*, 2007; Wallner *et al.*, 2012).

Table 6: k_{cat} – values of BBE wild type and different variant proteins.

Protein	k_{cat} (sec^{-1})
BBE WT	8.0 ± 0.2
His174Asn	1.18 ± 0.08
His174Ala	0.067 ± 0.01
Trp165Phe	10.1 ± 2

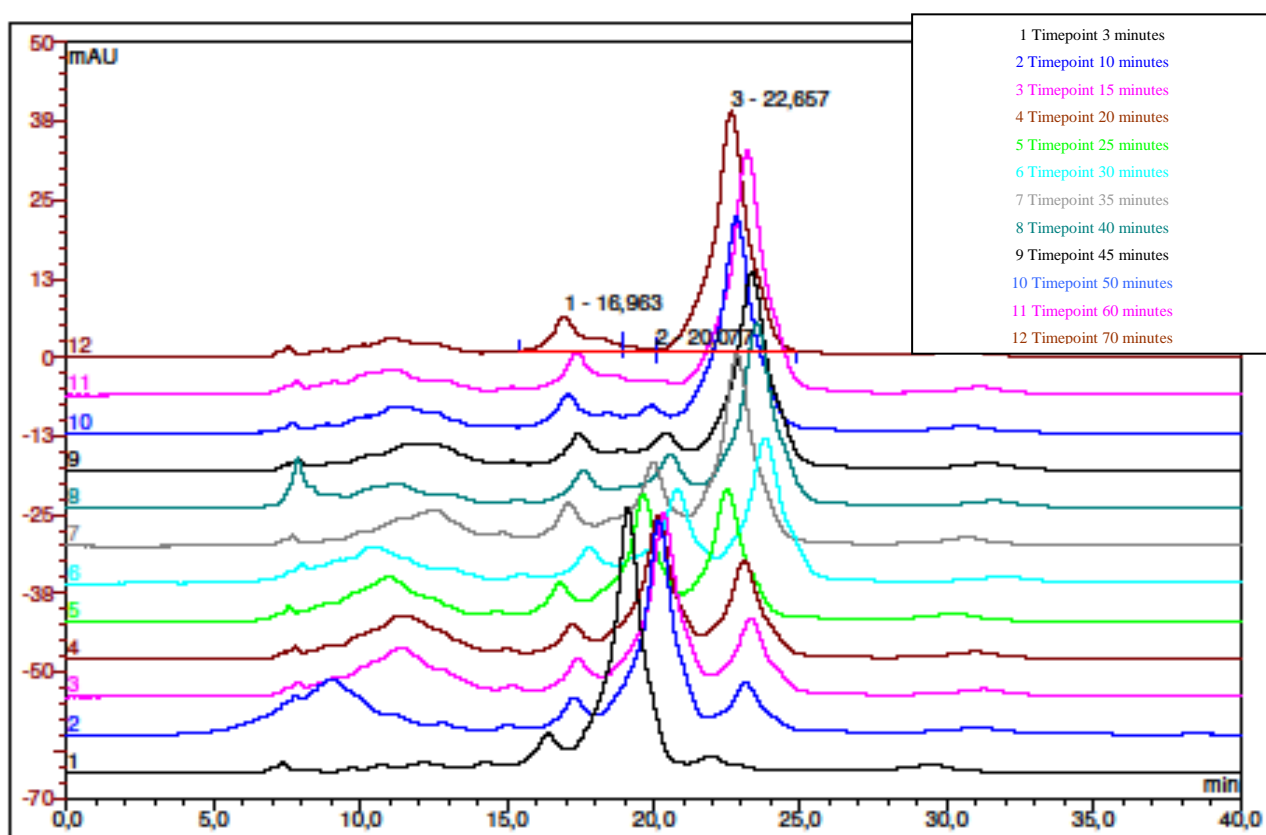


Figure 26: HPLC profile of the BBE His174Asn-catalysed conversion of (*S*)-reticuline to (*S*)-scoulerine.

The steady-state turnover rate of BBE His174Asn was determined using high performance liquid chromatography analysis of substrate conversion.

Figure 25 shows the conversion of (*S*)-reticuline to (*S*)-scoulerine at different time points. (*S*)-reticuline and (*S*)-scoulerine exhibit retention times of 17 and 22 minutes, respectively. Turnover rates were calculated from the initial velocity of the catalytic reaction.

4.2.3 Redox potential determination

This analysis was performed using a Stopped-Flow device and applying the dye-equilibrium method. Reduction was achieved by the xanthine/xanthine oxidase system in the presence of a redox mediator. 8.6 μM BBE His174Asn was reduced by xanthine/xanthine oxidase system in the presence of thionine acetate. Thionine acetate was used as dye, which has a midpoint potential of $E_M = 64$ mV at 25 $^\circ\text{C}$ and pH 7.0. The parallel reduction of the protein and redox dye was followed spectrophotometrically with a diode-array detector. Plotting $\log(\text{His174Asn}_{\text{ox}}/\text{His174Asn}_{\text{red}})$ versus $\log(\text{dye}_{\text{ox}}/\text{dye}_{\text{red}})$ allowed the estimation of redox potentials.

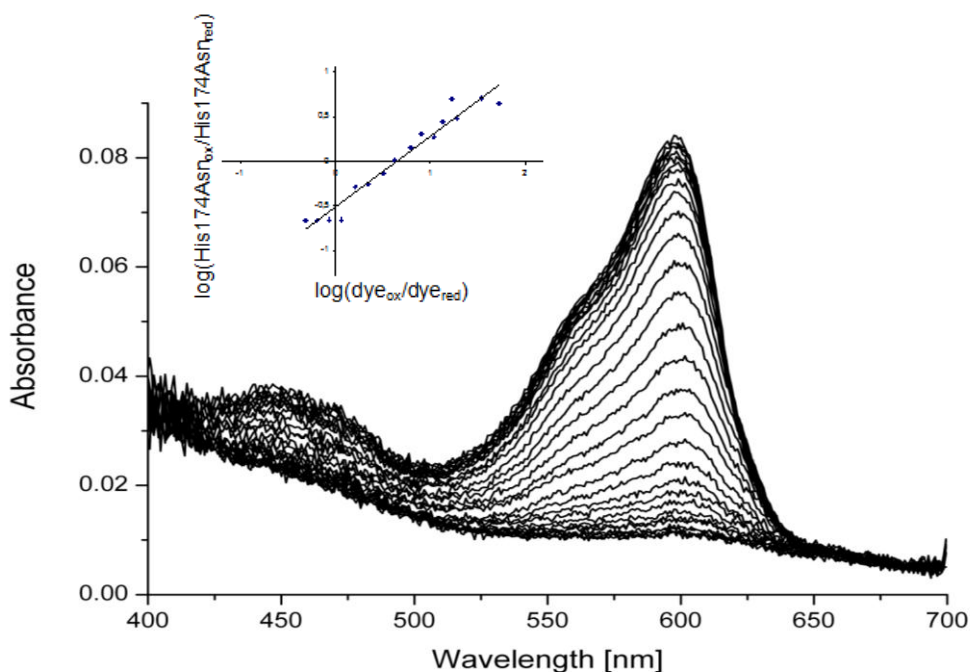


Figure 27: Redox potential determination of BBE His174Asn. Solid lines represent parallel reduction of protein BBE His174Asn and thionine acetate. The small inlay diagram represents the logarithmic determination of redox potential by plotting $\log(\text{His174Asn}_{\text{ox}}/\text{His174Asn}_{\text{red}})$ versus $\log(\text{dye}_{\text{ox}}/\text{dye}_{\text{red}})$.

Table 7: Redox potentials determination of BBE wild type and different variants.

Protein	E_0 (mV)
BBE WT	132 ± 4
H174N	75 ± 3
H174A	44 ± 3

The redox potential of BBE His174Asn was calculated to be 75 ± 3 mV.

The measurement was repeated ten times and to prove equilibrium between dye and flavin cofactor different amounts of electron delivering xanthine and xanthine oxidase were used. Therefore, complete reduction was achieved in 30 minutes to 2 hours.

4.2.4 Observation of flavin degradation

This experiment was additionally done to observe the changes in absorbance spectrum of the flavin cofactor during protein storage at 4 °C.

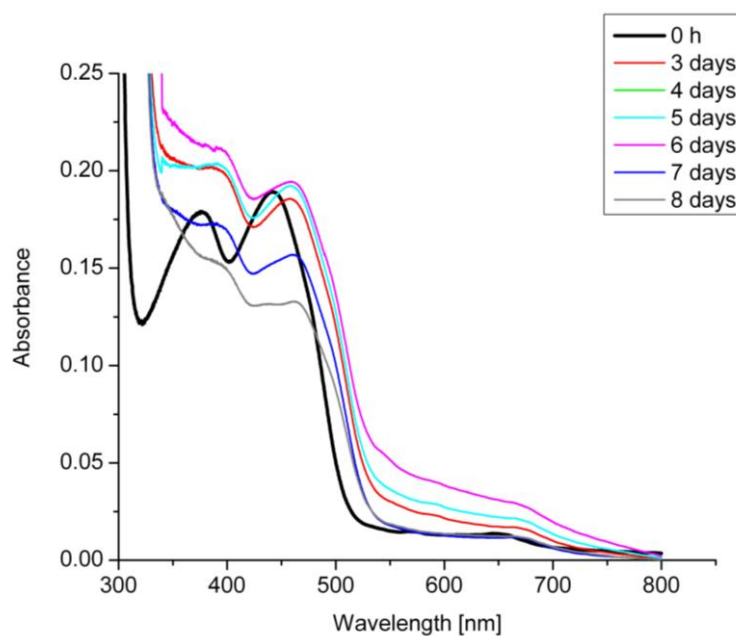


Figure 28: Flavin spectra recorded after various days. *Black solid line* shows the measurement directly after protein purification. *Solid coloured lines* show degradation of cofactor upon storage at 4 °C.

Figure 27 shows the degradation of the flavin cofactor. Measurements show that the flavin cofactor is slowly degraded when stored at 4 °C. Cofactor degradation was already monitored for BBE wild type and various variant proteins. Interestingly, degradation of the wild type enzyme seemed to occur much faster than degradation of BBE His174Asn.

4.2.5 Crystallization

Crystals formed under different conditions in micro batch experiments using the screen described in chapter 3: Methods. Up to now thin needles were formed under various conditions.

Table 8: Successful conditions for crystallization (Index Screen Protocol from Hampton).

Acronym	Condition
A2	2.0 M Ammonium sulfate, 0.1 M Sodium acetate trihydrate pH 5.0
A3	2.0 M Ammonium sulfate, 0.1 M BIS-TRIS pH 6.0
A4	2.0 M Ammonium sulfate, 0.1 M BIS-TRIS pH 7.0
A5	2.0 M Ammonium sulfate, 0.1 M HEPES pH 8.0
B6	1.4 M Sodium phosphate monobasic monohydrate/Potassium phosphate dibasic pH 6.9
B7	1.4 M Sodium phosphate monobasic monohydrate/Potassium phosphate dibasic pH 8.2
B9	1.8 M ammonium citrate tribasic pH 7.0
B10	0.8 M Succinic acid pH 7.0
B11	2.1 M DL-Malic acid pH 7.0
C3	2.4 M Sodium malonate pH 7.0
C4	35% v/v Tascimate pH 7.0
C5	60% v/v Tascimate pH 7.0
C7	0.8 M Potassium sodium tartrate tetrahydrate, 0.1 M Tris pH 9.0, 0.5% w/v Polyethylene glycol monomethyl ether 5,000
C8	1.0 M Ammonium sulfate, 0.1 M BIS-TRIS pH 6.0, 1% w/v Polyethylene glycol 3,350
C9	1.1 M Sodium malonate pH 7.0, 0.1 M HEPES pH 7.0, 0.5% v/v Jeffamine ED-2001 pH 7.0
C11	1.0 M Ammonium sulfate, 0.1 M HEPES pH 7.0, 0.5% w/v Polyethylene glycol 8,000
C12	15% v/v Tascimate pH 7.0, 0.1 M HEPES pH 7.0, 0.2% v/v Polyethylene glycol 3,350
F8	0.2 M Ammonium sulfate, 0.1 M HEPES pH 8.0, 25% w/v Polyethylene glycol 3,350
G3	0.2 M Lithium sulfate monohydrate, 0.1 M BIS-TRIS pH 7.0, 25% w/v Polyethylene glycol 3,350
G4	0.2 M Lithium sulfate monohydrate, 0.1 M HEPES pH 8.0, 25% w/v Polyethylene glycol 3,350
G5	0.2 M Lithium sulfate monohydrate, 0.1 M Tris pH 9.0, 25% w/v Polyethylene glycol 3,350
H10	0.2 M Sodium citrate tribasic dihydrate, 20% w/v Polyethylene glycol 3,350

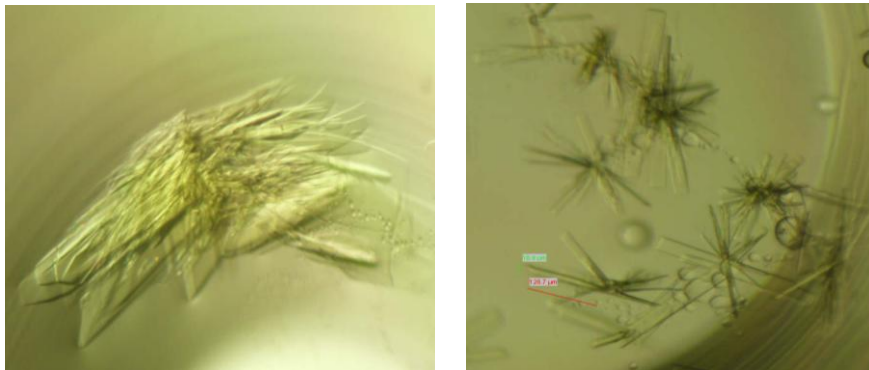


Figure 29: Needles formed using conditions A5 (left) and B6 (right) of the Index Screen Protocol from Hampton.

5 Discussion

The primary task of this work was to express a new protein variant of BBE in order to evaluate oxygen reactivity of this enzyme. For this reason His174 was replaced with Asn. From sequence alignments it is known that His174 of BBE is strictly conserved among bicovalently linked flavoprotein oxidases and that an asparagine residue is present at the respective position of bicovalently flavinylated dehydrogenases. Today known examples of bicovalently flavinylated dehydrogenases are TrdL from *Streptomyces sp.* or Phl p 4, a pollen allergen from timothy grass. Thus, the aim of this project was to transform BBE from an oxidase to a dehydrogenase through exchange of histidine with asparagine.

P. pastoris was chosen as host for heterologous protein expression. Using large-scale protein production in a bioreactor, 115 mg of protein were expressed in a 7 L fermenter.

First of all expression level was influenced by the expression method applied. When the results of expression in shake flasks are compared with expression yields in bioreactor, it is obvious that expression in large scale with strict process control is more reproducible and efficient compared to shake flasks.

Shake flasks with and without grooves did not lead to the expression of sufficient amounts of His174Asn. A probable reason for the poor protein expression is the lack of control of critical parameters like oxygen level and constant substrate feed. In large scale protein production all process parameters are automatically controlled and set to desired values.

As expected, the expressed protein was found in the supernatant, and was purified via hydrophobic interaction chromatography. In case of expression in shake flasks, not enough protein was expressed for a successful purification using HIC. Protein yields from large scale expression were high enough for obtaining pure protein for biochemical characterisation.

Protein expression using the secretory machinery of *P. pastoris* facilitates protein purification. BBE His174Asn was successfully secreted into the fermentation medium and thus no cell lysis was necessary to release intracellular protein. The fermentation medium containing all secreted protein was directly used for the first purification step via HIC. This step was performed to concentrate the protein and to remove parts of the protein impurities.

Consecutively, a gelfiltration step was performed for removing further impurities.

Anionic exchange chromatography was finally performed to obtain highly pure protein, which was also used for crystallization.

Although there is no crystal structure available for BBE His174Asn at the moment, the spectra of oxidized and reduced enzyme strongly suggest the presence of a bicovalently linked flavin cofactor.

Moreover, BBE His174Asn was biochemically characterized in order to determine the effect of the amino acid exchange on kinetic properties and the redox potential of His174Asn.

A noticeable effect of the His174Asn replacement was observed for different kinetic parameters such as steady-state turnover rate and redox potential. An approximately 7-fold decrease in catalytic activity compared to the wild type BBE was determined for His174Asn. On the other hand the decrease was much more pronounced for His174Ala (approximately 120-fold compared to wild type). On this way we could confirm that His174 is required for effective catalysis and that the replacement of His with Ala shows a more pronounced effect compared to His174Asn.

From the crystal structure of wild type BBE it is obvious that His174 cannot directly interact with the flavin isoalloxazine ring but is involved in a hydrogen bonding network through interaction with the C2' hydroxyl group of the ribityl side chain of the flavin. This hydroxyl group again interacts with N(1)-C(2)=O locus of the isoalloxazine ring system. (Wallner *et al.*, 2012).

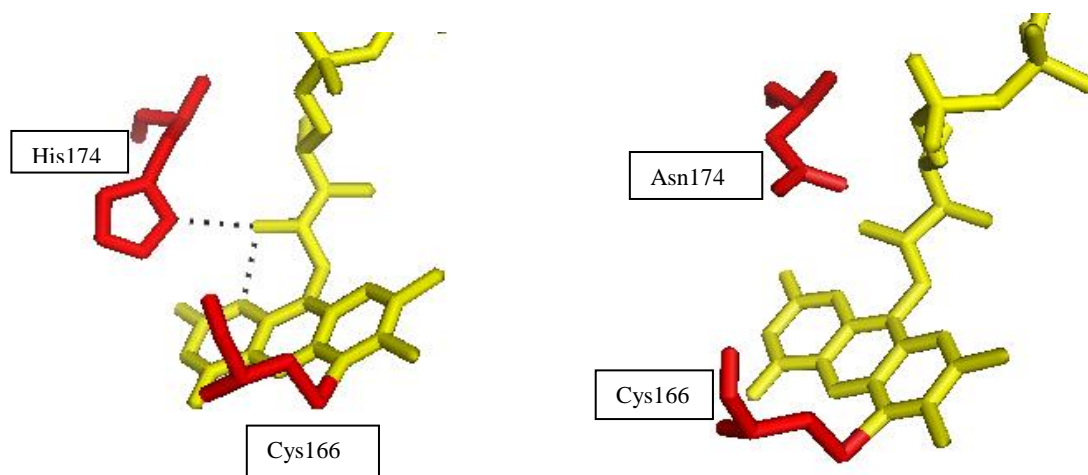


Figure 30: Hydrogen bonding network between amino acids and isoalloxazine ring of the flavin cofactor. Left: Bonding network between His174 and flavin cofactor. Right: Possible position of new amino acid Asn.

This hydrogen bonding network is crucial for stabilizing transiently formed negative charges at the N(1)-C(2)=O locus. Thus, it is possible that this hydrogen bonding network can not form completely and the resulting lack in stabilization of anionic forms of the flavin cofactor could explain the decrease in k_{cat} value and the 2-fold decrease in redox potential of the His174Asn variant in comparison with wild type BBE. Interestingly, the redox potential of BBE His174Asn (75 ± 3 mV) is still higher compared to the His174Ala variant (44 ± 3 mV). This confirms that replacing His174 with Ala has a stronger effect than the replacement with Asn. A possible explanation is that Ala is an amino acid with a side chain that does not form hydrogen bonds. For an His174Asn variant hydrogen bonding is still possible, however a crystal structure of BBE His174Asn would be necessary to prove this assumption.

Table 9: Comparison of BBE WT and His174Asn and His174Ala variant proteins

Protein	k_{cat} (sec^{-1})	E_0 (mV)
BBE WT	8.0 ± 0.2	132 ± 4
His174Asn	1.18 ± 0.08	75 ± 3
His174Ala	0.067 ± 0.01	44 ± 3

Interesting observations were also made upon photoreduction of the His174Asn variant. When His174Asn was completely reduced by photoirradiation, the formation of a thio-flavin product as characterised by the broad absorption around 800 nm was observable after reoxidation upon admission of oxygen (see figure 24). This indicates an irreversible bond breakage.

The same happened when wild type BBE was completely reduced by photoirradiation, also here formation of 6-thio FAD was observable.

In case of His174Ala, no 6-thio FAD was detected, which can be attributed to a lack of stabilisation of the modified flavin. Here the full reduction of the flavin cofactor resulted in a cleavage of the C6-sulfur bond instead of the formation of a thio-flavin.

On the other hand if BBE His174Asn is not fully reduced, no formation of thio-flavin was observable. But, one additional step in photoirradiation leads to formation of thio product. This means that bond breakage between cysteine residue and isoalloxazine ring system happens much faster which leads to formation of thio-flavin product.

Furthermore, protein stability was monitored when BBE His174Asn was stored at 4 °C. Through photometric measurements it was possible to determine the presence of the colourless 4a-spirohydantoin degradation product. It was already known that 4a-spirohydantoin forms in BBE wild type since electron density for this degradation product was found in the wild type structure (Winkler *et al.*, 2008).

The formation of 4a-spirohydantoin can be explained through hydrolysis of the flavin cofactor. BBE WT has a flavin cofactor that is more nucleophilic than the cofactor of His174Asn. Therefore it is much easier for water molecules to hydrolyse the flavin ring of BBE WT compared to His174Asn. This could be also confirmed by stability studies on BBE WT compared to His174Asn. This could be also confirmed by stability studies on BBE His174Asn. Degradation of this variant protein seemed to occur much slower as compared to the wild type enzyme.

Spirohydantoin formation was also observed for W165F. In case of W165F degradation of the flavin cofactor occurred very rapidly. This could be explained by the difference in size of tryptophan and phenylalanine. When tryptophan is exchanged with phenylalanine there is much more free space for water molecules which access the active site and hydrolyse the flavin cofactor. Moreover, the redox potential of BBE W165F is in the range of the wild type enzyme and thus nucleophilicity of the flavin cofactor might be similar for BBE wild type and BBE W165F. This could explain the increased spirohydantoin formation in W165F.

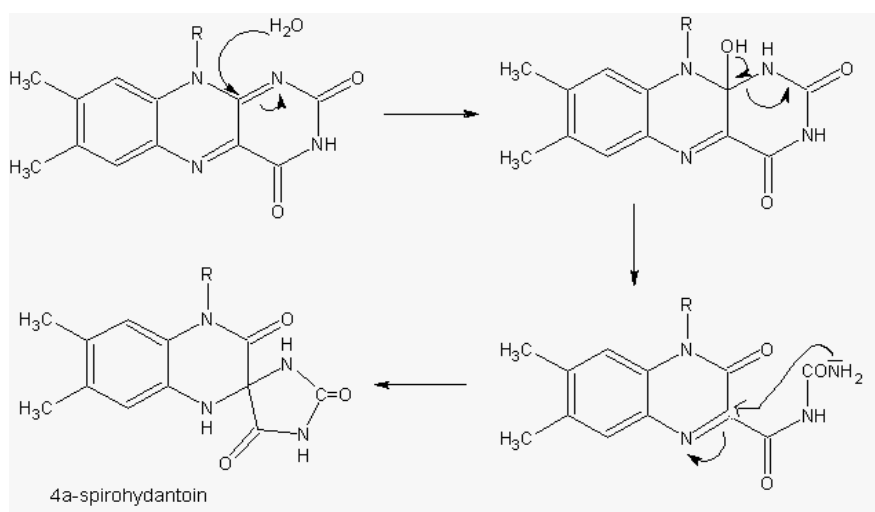


Figure 31: Potential mechanisms of 4a-spirohydantoin formation.

From previous studies on BBE it was already known that BBE crystals form best in seeding experiments. Unfortunately, no seeding crystals were available for this study, therefore first crystallization trials were performed using the buffer condition, which was optimal for wild type BBE.

Moreover, crystallization screens were prepared for His174Asn using the Index Screen Protocol from Hampton. After almost one month first needles were detected in some of the crystallization trials (see figure 28), however, these needles could not be used for collecting diffraction patterns.

6 Conclusion

Our results have shown that His174 is a crucial active site residue in BBE. It plays an important role in the stabilisation of the reduced form of the flavin by maintaining a hydrogen bonding network via the C2` hydroxyl residue of the ribityl chain.

It was possible to show that replacement of His174 destabilizes the reduced state of flavin cofactor and to confirm that His174 is crucial for stabilizing the negative charge of the isoalloxazine ring.

Decrease in redox potential and in turnover rate, in comparison to wild type BBE, shows that the hydrogen bonding network with His174 and the C2`hydroxyl group of the ribityl chain of the flavin is crucial for stabilizing a negative charge at the N(1)-C(2)=O locus. In case of His174Ala variant exchange of His with Ala leads to more pronounced decrease in redox potential and turnover rates, because the hydrogen bonding network between His and isoalloxazine ring system does not exist any more.

Asparagine, on the other hand, is still capable of participating in a hydrogen bonding network. Therefore, the decrease in redox potential and turnover rates seems to be less pronounced.

However, for further understanding of the effect of the amino acid replacement in BBE His174Asn the crystal structure of this variant would be necessary.

Moreover, to see if the replacement of amino acids led to transformation of oxidase into the dehydrogenase, k_{ox} and k_{red} needs to be determined on Stopped-Flow device.

7 Appendix 1

BBE-like from *Arabidopsis thaliana*

7.1 Introduction

During this master thesis not only expression and characterization of BBE His174Asn was performed, I also contributed to studies on BBE-like enzymes in *Arabidopsis thaliana*. From sequence alignments it was known that *Arabidopsis thaliana* possesses 28 genes with homology to BBE (therefore these genes are named BBE-like).

These 28 homologous proteins were analysed using the YASARA modelling tool with special regard to the amino acids in the active site and the residues that are required to form the bivalent attachment. Several candidates with interesting motifs for covalent cofactor attachment were chosen for heterologous expression for further investigations. Those candidates were BBE-like 10, BBE-like 15, BBE-like 27, and BBE-like 28 (Wallner *et al.*, 2012a).

Table 10: Sequence alignment for BBE-like 10, 15, 27, and 28

Name	Comparison to BBE Active Site Residues							
	His104	Cys166	Glu417	Tyr106	His459	His174	Tyr456	Trp165
BBE-like 10	His	Ser	Glu	Phe	---	His	---	Leu
BBE-like 15	His	Cys	Gln	Tyr	---	His	---	Leu
BBE-like 27	His	Tyr	Gln	Tyr	Phe	Gln	Tyr	Leu
BBE-like 28	His	His	Gln	Tyr	Phe	Gln	Tyr	Ile

For those proteins, gene constructs were made to enable the protein expression in large scale amounts. I contributed to this project by doing the cloning of the expression constructs.

7.2 BBE-like proteins in plants

The family of BBE-like proteins is increasing. The sequence alignments give evidence that many plant proteins possess conserved histidine and cysteine residues which is responsible for bivalent attachment of the cofactor. Using Blast tool from phytozome website

(<http://www.phytozome.net/search.php>) it was possible to target 26 plant species with BBE-homologues. Those plants can be seen in table 8.

Table 11: BBE-like proteins in different plants and plant families (Wallner *et al.*, 2012a).

Plant	Family	Common name	BBE-like homologues
<i>Populus trichocarpa</i>	<i>Salicaceae</i>	Western balsam poplar	57
<i>Glycine max</i>	<i>Fabaceae</i>	soybean	46
<i>Citrus clementina</i>	<i>Rutaceae</i>	clementine	39
<i>Prunus persica</i>	<i>Rosaceae</i>	peach	30
<i>Arabidopsis thaliana</i>	<i>Brassicaceae</i>		28
<i>Arabidopsis lyrata</i>	<i>Brassicaceae</i>		27
<i>Eucalyptus grandis</i>	<i>Myrtaceae</i>	eucalyptus	27
<i>Mimulus guttatus</i>	<i>Scrophulariaceae</i>	common monkey-flower	25
<i>Citrus sinensis</i>	<i>Rutaceae</i>	orange	24
<i>Cucumis sativus</i>	<i>Cucurbitaceae</i>	cucumber	23
<i>Aquilegia coerulea</i>	<i>Ranunculaceae</i>	Rocky mountain columbine	18
<i>Medicago truncatula</i>	<i>Fabaceae</i>	barrel medic	18
<i>Manihot esculenta</i>	<i>Euphorbiaceae</i>	cassava (manioc)	17
<i>Zea mays</i>	<i>Poaceae</i>	maize	16
<i>Ricinus communis</i>	<i>Euphorbiaceae</i>	ricinus	15
<i>Setaria italica</i>	<i>Poaceae</i>	foxtail millet	13
<i>Sorghum bicolor</i>	<i>Poaceae</i>	sorghum	13
<i>Carica papaya</i>	<i>Caricaceae</i>	papaya	12
<i>Oryza sativa</i>	<i>Poaceae</i>	rice	11
<i>Brachypodium distachyon</i>	<i>Poaceae</i>	purple false brome	10
<i>Vitis vinifera</i>	<i>Vitaceae</i>	grape	5
<i>Physcomitrella patens</i>	<i>Funariaceae</i>		1
<i>Chlamydomonas reinhardtii</i>	<i>Chlamydomonadaceae</i>		0
<i>Selaginella moellendorffii</i>	<i>Selaginellaceae</i>		0
<i>Volvox carteri</i>	<i>Volvocaceae</i>		0

Flavoproteins with bicovalently attached cofactor which can be found in plants are involved in many different processes. Some of them comprise oxidases in alkaloid biosynthesis like BBE and STOX. Other flavoproteins are involved in cannabinoid metabolism (THCA syntase) or in plant defense against different pathogens like nectarin V

from *Helianthus annuus* and *Lactuca sativa*. A further group of bicovalently linked plant proteins act as pollen allergens like Phl p 4 (Nandy *et al.*, 2005).

In *Papaveraceae* flavoproteins with bicovalently linked cofactors are capable to catalyze important oxidations in alkaloid biosynthesis. As already mentioned, BBE catalyses the unique formation of the methylene bridge of (*S*)-scoulerine in poppy plants (Winkler *et al.*, 2006).

Not all flavoproteins with bicovalently linked cofactors are responsible for production of secondary metabolites in plants. Some of them, like nectarin V (NEC5), are expressed in the nectar gland of tabaco plant. This enzyme possesses glucose oxidase activity. It is capable to oxidize glucose to gluconolactone and hydrogen peroxide. Hydrogen peroxide plays a important role in defense against microbial attack by preventing contaminations of the floral reproductive tract (Carter and Thornburg, 2004).

Another group of BBE-like proteins is known to act as pollen allergens. They share the histidine and cysteine residues which are important for covalent flavinylation. Those allergens are generally found in grasses and different types of corn. Phl p 4, which is homologous to BBE, was discovered in two isoforms in timothy grass and the crystal structure confirmed the biocovalent attachment of the FAD cofactor (Dewitt *et al.*, 2006).

Mentioned examples of characterized BBE-like proteins show that this group of flavoenzymes with bicovalently linked cofactors is involved in many chemical reactions and different biological functions (Wallner *et al.*, 2012a).

On the other hand, specific enzyme functions can not be predicted only on the basis of sequence homology. This suggestion has been confirmed by various examples like ChitO from *F. graminearum*. Substrate specificity of this enzyme was changed by a replacement of a single amino acid in the active site, which led to increased acceptance of glucose and small oligosaccharides (Heuts *et al.*, 2007).

Interestingly, also *A. thaliana* seems to possess flavoproteins with biocovalently linked cofactors. To identify them, the BBE sequence from *E. californica* was used for a Blastp search. This search was done against the whole *Arabidopsis* genome which led to the

discovery of 28 BBE homologues in *A. thaliana*. All of them are encoded on chromosomes 1, 2, 4, and 5 (Wallner *et al.*, 2012a).

Using YASARA modelling tool it was possible to analyse all 28 homologs of *A. thaliana*. All of them possess a conserved histidine residue on the site corresponding to His104 of BBE which indicates a covalent 8 α -histidinyl linkage of the cofactor. Moreover, 24 of them possess the conserved cysteine residue for 6-S-cysteinylation, which means that 24 of them are most likely bicovalent flavoenzymes. The remaining four homologs (BBE-like 10, 25, 27, and 28) have tyrosine, serine or histidine residue at the position corresponding to Cys166 of BBE (Wallner *et al.*, 2012a).

7.3 Conclusion

In the last few years it was discovered that ~ 25% of all flavoproteins with covalently linked cofactors feature bicovalent flavinylation. A large number of bacterial, fungal and plant genes belong to the family of “BBE-like proteins”. Up to now, bicovalent attachment was discovered in plants, bacteria and fungi. Some of them are rich in bicovalent flavoproteins and others appear to have only few members of this family.

In plants, bicovalent flavoproteins are able to catalyse cyclization reactions in natural products like alkaloid and terpen biosynthesis. As sugar oxidases those enzymes are involved in plant and fungal defense against pathogens. On the other hand, as alcohol oxidases they are able to catalyse final steps in antibiotic biosynthesis in bacteria (Wallner *et al.*, 2012a).

Sequence alignments supports the theory that some BBE homologues in *A. thaliana* are carbohydrate oxidases. In plants these enzymes play important role in active plant defense because they are capable to produce hydrogen peroxide as a product of enzymatic turnover. Some BBE homologs in *A. thaliana* which acts as carbohydrate oxidases are involved in floral defense against different plant pathogens (Wallner *et al.*, 2012a).

7.4 Results

It was possible to make expression constructs for four BBE-like genes of *A. thaliana*. The cloning was performed as described in chapter 3: Methods.

PCR reactions were performed to amplify the DNA. This can be seen in figure 29.

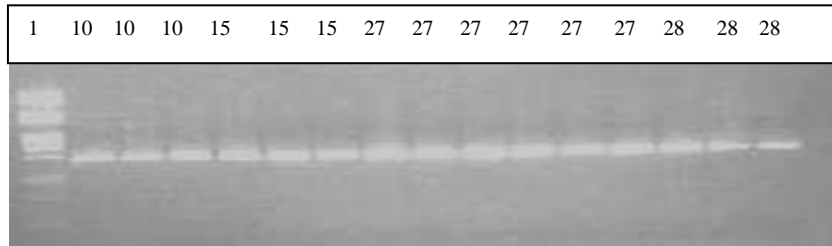


Figure 32: PCR products of BBE-like 10, 15, 27 and 28. Lane 1: λ -DNA digested with *Pst* I (from Fermentas); Lanes 10, 15, 27 and 28: PCR products for each construct. All products are in the range of 1.7 kb.

Restriction of PCR products was performed over night. Insert (BBE-like) and vector (pPICZalpha) were ligated and the generation of the desired expression constructs was verified by control restriction and plasmid sequencing.

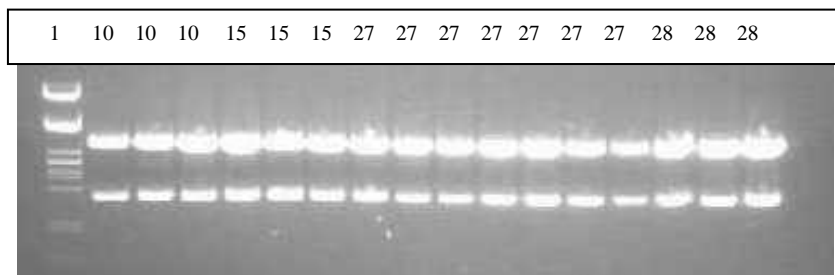


Figure 33: Control restriction of BBE-like 10, 15, 27, and 28. Lane 1: λ -DNA digested with *Pst* I (from Fermentas); Lanes 10, 15, 27 and 28: control restriction of ligated constructs. Upper lanes represent pPICZalpha vector with 3.5 kb. Lower lanes represent BBE-like inserts with 1.7 kb.

As it can be seen from figure 30, the cloning of BBE-like inserts into pPICZalpha vector was successful. Expression cassettes were linearised with *Sac* I enzyme and then transformed into *Pichia pastoris* KM71H strain and a strain that coexpresses PDI.

Further expression and characterisation of BBE-like proteins was done by Bastian Daniel.

8 Appendix 2

Figure 1: Structure and numbering conventions of benzylisoquinoline alkaloids	2
Figure 2: Summary of alkaloid biosynthesis.	3
Figure 3: Types of covalent flavin linkage found in flavoenzymes.	6
Figure 4: Schematic representation of the structure of active site of BBE.....	13
Figure 5: Overall reaction catalysed by BBE	14
Figure 6: Proposed reaction mechanism for the BBE-catalyzed reaction	16
Figure 7: pPICZalpha vector	23
Figure 8: LMW standard for SDS-gels.....	28
Figure 9: Control gel after mutagenesis PCR.....	33
Figure 10: Dot Blot for H174N.....	34
Figure 11: Purification of H174N PDI F3 via hydrophobic interaction chromatography	35
Figure 12: SDS Gel of the course of expression of WT G8	36
Figure 13: SDS Gel of the course of expression of PDI F3	36
Figure 14: Fermentation of <i>P. pastoris</i> KM71H [pPICZalpha-BBE His174Asn].	37
Figure 15: Purification of BBE His174Asn using hydrophobic interaction chromatography.	38
Figure 16: Activity assay after purification via HIC column.	39
Figure 17: SDS PAGE of fractions from purification of His174Asn via HIC	39
Figure 18: Size exclusion chromatography as second step for the purification of BBE His174Asn.	40
Figure 19: Representative SDS-gel of fractions after size exclusion chromatography.	40
Figure 20: Concentrated fractions after gel filtration.....	41
Figure 21: Final purification step via ion exchange chromatography.....	42
Figure 22: Absorbance spectrum of BBE His174Asn.	43
Figure 23: Selected spectra of the complete photoreduction of BBE His174Asn.....	44
Figure 24: Reoxidation upon admission of oxygen.	44
Figure 25: Unfinished photoreduction of BBE His174Asn	45
Figure 26: HPLC profile of the BBE His174Asn-catalysed conversion of (S)-reticuline to (S)-scoulerine. ...	46
Figure 27: Redox potential determination of BBE His174Asn.....	47
Figure 28: Flavin spectra recorded after various days.....	48
Figure 29: Needles formed using conditions A5 (left) and B6 (right) of the Index Screen Protocol.....	50
Figure 30: Hydrogen bonding network between amino acids and isoalloxazine ring of the flavin cofactor. .	52
Figure 31: Potential mechanisms of 4a-spirohydantoin formation.....	54
Figure 32: PCR products of BBE-like 10, 15, 27 and 28.	61
Figure 33: Control restriction of BBE-like 10, 15, 27, and 28.....	61

8.1 List of tables

<i>Table 1: Buffers and solutions for SDS-polyacrylamid gel electrophoresis.</i>	20
<i>Table 2: Pichia strains used in this master thesis.</i>	22
<i>Table 3: Vectors used in this master thesis.</i>	22
<i>Table 4: Program used for Colony PCR.</i>	29
<i>Table 5: Photometric determination of protein concentration.</i>	42
<i>Table 6: k_{cat} – values of BBE wild type and different variant proteins.</i>	46
<i>Table 7: Redox potentials determination of BBE wild type and different variants.</i>	48
<i>Table 8: Successful conditions for crystallization (Index Screen Protocol from Hampton).</i>	49
<i>Table 9: Comparison of BBE WT and His174Asn and His174Ala variant proteins</i>	53
<i>Table 10: Sequence alignment for BBE-like 10, 15, 27, and 28.</i>	57
<i>Table 11: BBE-like proteins in different plants and plant families</i>	58

9 References

- Anselmi, E., Fayos, G., Blasco, R., Candenas, L., Cortes, D., and D'Ocon (1992), *P. J. Pharm. Pharmacol.* **44**, 337-343.
- Carter, C.J., and Thornburg, R.W. (2004), *Plant Physiol.* **134**:460-9
- Chao, J., Lu, T. C., Liao, J. W., Huang, T. H., Lee, M. S., Cheng, H. Y., Ho, L. K., Kuo, C. L., and Peng (2009), *W. H. J. Ethnopharmacol.* **125**, 297-303.
- Dewitt, A.M., Andersson, K., Peltre, G., and Lidholm, J. (2006), *Clin Exp Allergy*, **36**:77-86.
- Dittrich, H. and Kutchan, T.M. (1991), *Proc.Natl.Acad.Sci.U.S.A* **88** (22), 9969-9973.
- Dreveny, I., Kratky, C. and Gruber, K. (2002), *Protein Science* **11** (2), 292-300.
- Edmondson, D.E. (1995), *Xenobiotica* **25** (7), 735-753.
- Facchini, P. J., Johnson, A. G., Poupart, J., and de Luca, V. (1996), *Plant Physiol.* **111**, 687-697.
- Facchini, P. J. (2001), *Annu. Rev. Plant Physiol. Plant Mol. Biol.* **52**, 29-66.
- Facchini, P. J., and St-Pierre, B.(2005), *Curr. Opin. Plant Biol.* **8**, 657-666
- Facchini, P., Hagel, J., Liscombe, D., Loukanina, N., MacLeod, B., Samanani, M., and Zulak, K.(2007), *Phytochen Rev.* **6**, 97-124.
- Fraaije, M.W. and Mattevi, A. (2000), *Trends in Biochemical Sciences* **25** (3), 126-132.
- Ghisla, S., and Thorpe, C. (2004), *European Journal of Biochemistry* **271** (3), 494-508.

Heuts, D.P., Janssen, D.B., and Fraaije, M.W.(2007), *FEBS Lett.* **581**:4905-9

Heuts D.P., Winter R.T., Damsma G.E., Janssen D.B., and Fraaije M.W.. (2008), *Biochem J.* **413** (1):175-83.

Heuts, D.P., Scrutton, N.S., McIntire, W.S., and Fraaije, M.W. (2009), *FEBS Journal* **276** (13):3405-27.

Huang, C. H., Lai, W. L., Lee, M. H., Chen, C. J., Vasella, A., Tsai, Y. C., and Liaw, S. H. J. (2005), *Biol. Chem.* **280**, 38831-38838.

Hung, T. M., Ngoc, T. M., Youn, U. J., Min, B. S., Na, M., Thuong, P. T., and Bae, K. (2008), *Biol. Pharm. Bull.* **31**, 159-162

Kashiwada, Y., Aoshima, A., Ikeshiro, Y., Chen, Y. P., Furukawa, H., Itoigawa, M., Fujioka, T., Mihashi, K., Cosentino, L. M., Morris-Natschke, S. L., and Lee, K.H. (2005), *Bioorg. Med. Chem.* **13**, 443-448.

Kitzing, K., Auweter, S., Amrhein, N. and Macheroux, P.(2004), *Journal of Biological Chemistry* **279** (10), 9451-9461

Kutchan, T.M., Bock, A. and Dittrich, H. (1994), *Phytochemistry* **35** (2), 353-360.

Liscombe, D. K., Macleod, B. P., Loukanina, N., Nandi, O. I., and Facchini, P. J. (2005), *Phytochemistry* **66**, 1374-1393

Liscombe, D. K., and Facchini, P. J.(2008), *Curr. Opin. Biotechnol.* **19**, 173-180

Macheroux, P., Kappes, B., and Ealick, S. E. (2011), *FEBS Journal* **278**, 2625-2634

Massey, V. (2000), *Biochemical Society Transactions* **28**, 283-296.

Mewies M, Basran J, Packman L.C., Hille, R, and Scrutton, N.S. (1997), *Biochemistry* **36** (23):7162-8

Minami, H., Kim, J. S., Ikezawa, N., Takemura, T., Katayama, T., Kumagai, H., and Sato, F. (2008), *Proc. Natl. Acad. Sci. U. S. A.* **105**, 7393-7398

Mo, J., Guo, Y., Yang, Y. S., Shen, J. S., Jin, G. Z., and Zhen, X. (2007), *Curr. Med. Chem.* **14**, 2996-3002

Mo, X., Huang, H., Ma, J., Wang, Z., Wang, B., Zhang, S., Zhang, C., and Ju, J. (2011), *Org. Lett.* **13**, 2212-2215

Morais, L. C., Barbosa-Filho, J. M., and Almeida, R. N., (1998), *J. Ethnopharmacol.*, **62**, 57-61

Nandy, A., Petersen, A., and Wald, M. (2005), *Biochem Biophys Res Commun* **337**:563-70

Palfey, B.A., McDonald, C.A., Fagan, R.L., Collard, F., and Monnier, V.M. (2011), *J. Am Chem Soc.* **133** (42):16809-11

Samanani, N., Park, S. U., and Facchini, P. J. (2005), *Plant Cell* **17**, 915-926

Steffens, P., Nagakura, N., and Zenk, M. H. (1984), *Tetrahedron Lett.* **25**, 951-952

Steffens, P., Nagakura, N. and Zenk, M.H. (1985), *Phytochemistry* **24** (11), 2577-2583

Tyler, V. E. (1994), *Haworth Press New York.*

Wallner, S., Winkler, A., Riedl, S., Dully, C., Horvath, S., Gruber, K., and Macheroux, P. (2012), *Biochemistry* **51**, 6139-6147

Wallner, S., Dully, C., Daniel, B., and Macheroux, P. (2012), *Handbook of Flavoproteins, Vol.1*, Walter De Gruyter, Berlin (editors Hille, R., Miller, S.M., Palfey, B.)

Winkler, A., Hartner, F., Kutchan, T. M., Glieder, A., and Macheroux, P. (2006), *J. Biol. Chem.* **281**, 21276-21285.

Winkler, A., Kutchan, T. M., and Macheroux, P. (2007), *J. Biol. Chem.* **282**, 24437-24443

Winkler, A., Łyskowski, A., Riedl, S., Puhl, M., Kutchan, T. M., Macheroux, P., and Gruber, K. (2008), *Nature Chemical Biology* **4**, 739-741

Winkler, A., Motz, K., Riedl, S., Puhl, M., Macheroux, P., and Gruber, K. (2009), *J. Biol. Chem.* **284**, 19993-20001

Wohlfahrt, G., Witt, S., Hendle, J., Schomburg, D., Kalisz, H. M., and Hecht, H. J. (1999), *Acta Crystallogr. D Biol. Crystallogr.* **55**, 969-977

Zhu, B., Peng, R.H., Fu, X.Y., Jin, X.F., Zhao, W., Xu, J., Han, H.J., Gao, J.J., Xu, Z.S., and Bian, L. (2012), *PLoS ONE* **Vol. 7**, Issue 7, e39861.